

# Use of electrophoretic impregnation and vacuum bagging to impregnate SiC powder into SiC fiber preforms

Binner, Jonathan; Vaidhyanathan, Bala; Jaglin, David; Needham, Sarah

DOI:

[10.1111/ijac.12143](https://doi.org/10.1111/ijac.12143)

License:

Other (please specify with Rights Statement)

*Document Version*

Peer reviewed version

*Citation for published version (Harvard):*

Binner, J, Vaidhyanathan, B, Jaglin, D & Needham, S 2013, 'Use of electrophoretic impregnation and vacuum bagging to impregnate SiC powder into SiC fiber preforms', *International Journal of Applied Ceramic Technology*, vol. 12, no. 1, pp. 212-222. <https://doi.org/10.1111/ijac.12143>

[Link to publication on Research at Birmingham portal](#)

## **Publisher Rights Statement:**

This article may be used for non-commercial purposes in accordance with Wiley Terms and Conditions for Self-Archiving.

## **General rights**

Unless a licence is specified above, all rights (including copyright and moral rights) in this document are retained by the authors and/or the copyright holders. The express permission of the copyright holder must be obtained for any use of this material other than for purposes permitted by law.

- Users may freely distribute the URL that is used to identify this publication.
- Users may download and/or print one copy of the publication from the University of Birmingham research portal for the purpose of private study or non-commercial research.
- User may use extracts from the document in line with the concept of 'fair dealing' under the Copyright, Designs and Patents Act 1988 (?)
- Users may not further distribute the material nor use it for the purposes of commercial gain.

Where a licence is displayed above, please note the terms and conditions of the licence govern your use of this document.

When citing, please reference the published version.

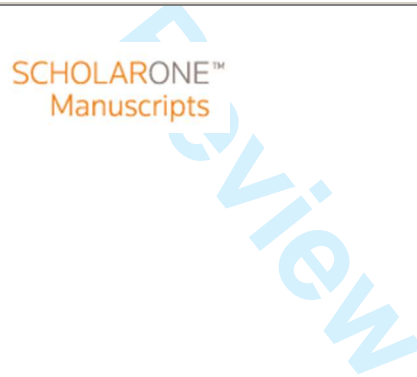
## **Take down policy**

While the University of Birmingham exercises care and attention in making items available there are rare occasions when an item has been uploaded in error or has been deemed to be commercially or otherwise sensitive.

If you believe that this is the case for this document, please contact [UBIRA@lists.bham.ac.uk](mailto:UBIRA@lists.bham.ac.uk) providing details and we will remove access to the work immediately and investigate.

**Use of Electrophoretic Impregnation and Vacuum Bagging  
to Impregnate SiC powder into SiC Fiber Preforms**

|                               |   |
|-------------------------------|---|
| Journal:                      | <i>International Journal of Applied Ceramic Technology</i>  |
| Manuscript ID:                | ACT-2148.R1   |
| Manuscript Type:              | Article   |
| Date Submitted by the Author: | n/a   |
| Complete List of Authors:     | Binner, Jon; Loughborough University, Materials;<br>Vaidhyanathan, Bala; Loughborough University, Materials<br>Jaglin, David; Loughborough University, Materials<br>Needham, Sarah; Rolls Royce plc, Civil Small & Medium Engines |
| Keywords:                     | infiltration, silicon carbide, composites, fibers   |
|                               |   |



1  
2  
3  
4  
5  
6  
7  
8  
9  
10  
11 **Use of Electrophoretic Impregnation and Vacuum Bagging to Impregnate SiC powder into**  
12 **SiC Fiber Preforms**  
13

14  
15  
16 Jon Binner<sup>\*</sup>, Bala Vaidhyanathan, David Jaglin and Sarah Needham<sup>†</sup>  
17

18  
19 Department of Materials, Loughborough University, Loughborough, Leicestershire LE11 3TU,  
20  
21 United Kingdom  
22

23  
24 **Abstract**  
25

26 Techniques based on vacuum bagging (VB) and electrophoretic impregnation (EPI) have been  
27 investigated for the impregnation of SiC powder into layered Nicalon SiC fabric preforms. The  
28 aim was to produce pre-impregnated samples for subsequent chemical vapour infiltration (CVI)  
29 with reduced intertow porosity that arises from the construction of the fabric layers whilst leaving  
30 unblocked the intratow porosity that is so indispensable for a successful infiltration. Since the  
31 goal was simply to learn about the ability to impregnate the samples, no interphase coating was  
32 applied to the fibers as would normally be used when producing SiC<sub>f</sub>-SiC composites. Whilst the  
33 VB process generally yielded much stronger preforms, depending on the pressure used and the  
34 powder particle size, it resulted in powder becoming located in the intratow rather than the  
35 intertow porosity. In contrast, provided an appropriate electrode arrangement was used, EPI  
36 offered the potential for a more controlled impregnation process with the powder primarily found  
37 in the intertow porosity; however, the preforms were very weak and delaminated easily. The  
38 combination of the two processes resulted in a very successful approach, with greater uniformity  
39 of particle infiltration and higher green strengths, whilst largely avoiding impregnating the  
40 intratow porosity.  
41  
42  
43  
44  
45  
46  
47  
48  
49  
50  
51  
52

53  
54 <sup>\*</sup> J.binner@Lboro.ac.uk

55 <sup>†</sup> Now with Rolls Royce plc., UK  
56  
57  
58  
59  
60

## I Introduction

SiC<sub>f</sub>/SiC composites are very promising materials for high temperature structural applications because of their good thermal stability and excellent mechanical properties. Of the various techniques used to produce fiber reinforced ceramic matrix composites, chemical vapour infiltration (CVI) has received considerable attention<sup>1-2</sup>. Combining isothermal or temperature gradient, isobaric or pressure gradient features, as well as the use of pulsing, CVI results in composites still containing 10 - 20% residual porosity<sup>3-6</sup> however. This is mainly due to two reasons: (i) when the minimum percolation threshold for transport through the pore structure is reached, infiltration becomes more and more difficult as the pore size decreases resulting in deposition occurring on the outside of the fiber network, and (ii) when the composite reaches a fractional density of ~70% the surface area becomes dominated by the macropores; these can take too long to infiltrate from a commercial viewpoint. It is the last 30% of densification that is financially costly because the infiltration time becomes extended (to days and even weeks in some cases) during this phase<sup>7</sup> and to produce fiber-reinforced ceramic matrix composites (FRCMCs) by any form of CVI at a commercially acceptable cost, the processing time must be kept short<sup>8</sup>.

As implied above, the porosity itself can be divided into two main types; fine intratow and much larger intertow porosity. In fibrous preforms densified up to 82% of theoretical<sup>9</sup>, the lamination of the plies combined with the weave design can result in intertow pores being as large as 0.3 to 0.6 mm in width and tens of millimetres long. There is also the problem of the packing of the fabric layer in the Z-direction<sup>10</sup>. Fig. 1a<sup>11</sup> provides an illustration of this type of porosity, which is the most harmful type of defect for mechanical properties as well as providing a path for corrosive agents. When present, these pores are very difficult to eliminate in fiber preforms produced from the lay-up of fiber sheets. In contrast, intratow pores are typically <15 μm in diameter and are formed when the matrix deposition on the individual fibers traps small pores,

1  
2  
3  
4  
5  
6  
7  
8  
9  
10  
11 Fig. 1b. Whilst some will probably always be residual after CVI-based processes, they are not  
12 considered to be particularly detrimental to the overall strength of the composite due to their  
13 small size<sup>9</sup>. Nevertheless, the elimination of this porosity by the use of the right infiltration  
14 conditions would also undoubtedly be desirable – provided it can be achieved without a  
15 significant increase in processing time and hence costs.  
16  
17  
18

19  
20  
21 Two-stage CVI processes have therefore been investigated where, under the right conditions,  
22 the initial stage sees the efficient filling of the finer, intratow porosity and the second stage seeks  
23 to fill as much of the coarser, intertow pores as possible within the economic limitations of the  
24 process<sup>12-13</sup>. For example, using marker layers, Lackey *et al.*<sup>14</sup> found that when using forced-flow  
25 CVI, intratow infiltration could be virtually complete within the first 2 h, although filling the intertow  
26 porosity took considerably longer. One potential problem with this approach is that some  
27 intertow porosity can become trapped in the structure when the intratow porosity becomes filled.  
28  
29  
30  
31  
32  
33

34  
35 Although not the focus of this paper, many other techniques are available for the fabrication of  
36 FRCMCs as well as CVI. For example, hot-pressing techniques have been used<sup>15</sup> in which the  
37 stacked green body was hot-pressed at up to 2023 K with a matrix consisting of  $\beta$ -SiC powder  
38 and sintering aids. Unfortunately, the composite displayed brittle behaviour even though Hi-  
39 Nicalon fibers were used. An approach based on slurry-cast melt infiltration with reaction-  
40 sintering<sup>16-18</sup> used a slurry consisting of SiC powder or a mixture of SiC powder and carbon  
41 powder in water that was impregnated into the SiC fiber preform. The green composite was then  
42 reaction sintered at 1720 K with melted silicon to obtain a rich SiC matrix. Disadvantages lay in  
43 the need for a designed mould and residual silicon metal as high as 15-20 vol.%, despite the low  
44 porosity achieved.  
45  
46  
47  
48  
49  
50  
51  
52

53  
54 An alternative approach can be based on the pre-impregnation of the macropores by a process  
55  
56  
57  
58  
59  
60

1  
2  
3  
4  
5  
6  
7  
8  
9  
10 other than CVI and polymer impregnation and pyrolysis (PIP) processes are very common and  
11 effective manufacturing techniques for high performance SiC<sub>f</sub>/SiC composites<sup>19-24</sup>. Six or more  
12 cycles of impregnations, followed by the pyrolysis, are typically required to achieve densities of  
13 80-85%. An important aspect of the process is that the matrix development affects the  
14 mechanical properties by inducing residual stresses due to shrinkage of the matrix during  
15 pyrolysis and also the anisotropy of the thermal expansion coefficient between the fibers and  
16 matrix<sup>25</sup>.  
17  
18  
19  
20  
21  
22  
23

24 The introduction of powder into the PIP was investigated by Gonon and Hampshire<sup>21</sup> who used  
25 polysilazane as precursor with the addition of Si<sub>3</sub>N<sub>4</sub> powder into SiC fiber preforms; 7 to 8 cycles  
26 of precursor impregnation and pyrolysis were required to reduce the porosity to approximately  
27 15%, but the presence of powder did not allow good cross-linking of the precursor and resulted  
28 in lower mechanical properties than the composite with the polymer alone, a result confirmed by  
29 Casadio<sup>23</sup>. Gotoh *et al.*<sup>20</sup> also pointed out that optimisation of the mechanical properties relies on  
30 the right volume of fiber and sintering aids. Fast heating techniques such as microwaves can be  
31 applied during the pyrolysis stage, providing time and energy savings since suitably high  
32 temperatures can be induced in a matter of minutes. Dong and co-authors<sup>24</sup> used this particular  
33 technique but required 8 cycles of impregnation to achieve a final density of 78%.  
34  
35  
36  
37  
38  
39  
40  
41  
42

43 Combining PIP with CVI allowed Kim *et al.*<sup>22</sup> to achieve an initial preform density of up to 70%  
44 after PIP, the subsequent isobaric, isothermal CVI step yielding a composite density of 82%.  
45 Ortona *et al.*<sup>10</sup> found that an initial CVI stage can prevent the swelling of the preform during the  
46 PIP stages.  
47  
48  
49  
50

51  
52 Two simple and rapid processes that have been shown to lead to a successful pre-impregnation  
53 in other, non-SiC fiber-based systems are vacuum bagging (VB) and electrophoretic  
54  
55  
56

1  
2  
3  
4  
5  
6  
7  
8  
9  
10  
11 impregnation (EPI). VB is a relatively simple process that was developed by Rolls Royce in the  
12 1980s for the preparation and/or repair of polymer matrix carbon fiber composites in the  
13 aerospace industry<sup>26-28</sup>. This technique has subsequently been modified for the impregnation of  
14 ceramic powders between tows and layers of fiber-based fabrics in order to reduce the porosity  
15 and improve the green strength<sup>29</sup>. The fabric layers are individually coated with ceramic slurry  
16 and stacked, prior to being dried and consolidated under vacuum. Process parameters are  
17 mainly associated with the preparation of the slurry, which controls the particle size being used  
18 and the amount of powder to be impregnated, and the pressure involved during vacuum  
19 bagging.  
20  
21  
22  
23  
24  
25  
26  
27

28 EPI is directly related the electrophoretic deposition process (EPD) wherein charged particles  
29 are deposited on an electrode surface via their migration under the action of an electrical field<sup>30</sup>.  
30 In the EPI process, a fiber preform is impregnated via the deposition of particles from a slurry  
31 onto individual cloth layers prior to assembly into the preform. The movement of ceramic  
32 particles in a suspension within an electric field is governed mainly by factors such as the field  
33 strength<sup>31</sup>, the pH of the suspension and its ionic strength<sup>32</sup>. The amount of polyelectrolyte  
34 addition also influences the rate of deposition and the homogeneity of the deposited material<sup>33</sup>.  
35 Green composite microstructures with good infiltration uniformity and few macro defects have  
36 been obtained by this technique<sup>34-35</sup> and previous work with a SiC<sub>f</sub>/SiC system resulted an  
37 increase in density from 20 vol.% (the initial fiber preform density) to over 40 vol.% in only 20  
38 minutes<sup>36</sup>.  
39  
40  
41  
42  
43  
44  
45  
46  
47  
48

49 In the present work, a methodical examination of the use of stand-alone VB and EPI techniques  
50 as well as their combination with a number of geometrical modifications has been undertaken  
51 with a view to producing SiC powder-loaded SiC fiber preforms that are suitable for subsequent  
52 infiltration with a SiC matrix using CVI. The goal was to fill the larger intertow pores, so reducing  
53  
54  
55  
56  
57  
58  
59  
60

1  
2  
3  
4  
5  
6  
7  
8  
9  
10  
11 the time that would be needed during a subsequent CVI stage, whilst avoiding the introduction of  
12 powder particles within the tows themselves. The particles can cause abrasion during use and  
13 damage the tows. In addition, it was desired to produce impregnated fiber preforms that were  
14 mechanically robust and capable of being handled prior to and during the CVI stage.  
15  
16  
17

## 18 19 **II Experimental procedure**

### 20 21 **(1) Materials**

22  
23 The preforms were made from NL-202 SiC fibers (Nippon Carbon, Tokyo, Japan) woven (by  
24 Sigmatec Ltd., UK) into a 2D plain weave NP1616 pattern. Forty eight mm circular discs were  
25 cut from the cloth using a metal template and ceramic scissors. The sizing agent was removed  
26 by heating the fiber discs in a furnace at 600°C for 2 h. Note, no attempt was made in this work  
27 to apply an interphase coating to the fibers prior to undertaking the impregnation with powder  
28 particles. This was because it was not believed that such a coating would materially affect the  
29 identification of the best choice of impregnation process, which was the goal of this work. For the  
30 impregnation experiments themselves, five SiC powders with mean particle sizes of  
31 approximately 0.6, 2.5, 6.7, 10.0 and 12.8  $\mu\text{m}$  were used; their details are provided in table 1.  
32  
33  
34  
35  
36  
37  
38  
39

### 40 41 **(2) SiC powder slurry preparation**

42  
43 Three types of slurries were prepared. Slurry A was used during the impregnation of preforms by  
44 vacuum bagging (VB), whilst slurries B and C were used for electrophoretic impregnation (EPI)  
45 and gravitational settling (GS).  
46  
47

48  
49 **Slurry A:** Aqueous slurries containing solids loadings between 20 and 40 vol.% were prepared  
50 for all five of the SiC powders. The powders were dispersed using 1 to 1.5 wt.% of Glascol K11  
51 (Ciba Speciality Chemicals, Bradford, UK) and the pH was fixed at  $9.0 \pm 0.2$  via the addition of  
52 ammonia solution. To eliminate powder agglomerates, the slurries were ball-milled in airtight  
53  
54  
55  
56



1  
2  
3  
4  
5  
6  
7  
8  
9  
10  
11 polyethylene bottles using zirconia media for 24 h, the viscosity being regularly monitored. Note  
12 that, although slurries with a solid loading higher than 45 vol.%, were prepared, problems were  
13 experienced with subsequent wetting of the fiber fabric and hence these slurries were discarded.  
14

15  
16 **Slurry B:** Ethanol-based slurries containing solids loadings of 5 and 10 vol.% were prepared for  
17 four of the SiC powders, the powders being dispersed using 0.5 vol.% of triethylamine (Ciba  
18 Speciality Chemicals, Bradford, UK); the pH was  $9.0 \pm 0.2$ . The 12.8  $\mu\text{m}$  SiC powder was not  
19 used as it was found that particle migration was difficult to achieve at the voltages used. To  
20 remove powder agglomerates, during preparation the slurries were exposed to ultrasonic energy  
21 at 23 kHz (Soniprep 150 Ultrasonicator, MSE Scientific Instruments, Manchester, UK) for a  
22 minimum of 60 s together with mechanical agitation using a magnetic stirrer.  
23  
24

25  
26 **Slurry C:** An identical preparation route as for slurry B was used to prepare aqueous  
27 suspensions containing 5 vol.% of SiC powders for all five of the SiC powders, again with the  
28 addition of ~0.5 vol.% of triethylamine. The pH was again  $9.0 \pm 0.2$ . Ultrasonic energy and  
29 mechanical agitation was again used, as described for slurry B.  
30  
31

### 32 33 34 35 36 37 38 (3) Vacuum bagging

39  
40 A small amount of slurry A was applied to the discs of SiC fabric using a nylon brush. Since the  
41 impregnation of the powder was performed manually, the VB technique potentially lacked  
42 repeatability with respect to the amount of powder deposited on each fabric layer. To minimise  
43 this problem each layer was weighed after brushing to ensure that a consistent amount had  
44 been deposited. Ten discs were then stacked and the layers compressed using a roller. Each  
45 preform was placed in the vacuum bagging equipment (Townsend & Mercer Ltd., Croydon, UK),  
46 Fig. 2a, and dried overnight at temperatures ranging from 20 to 60°C, a rotary pump being used  
47 to apply a vacuum of  $\sim 0.5 \times 10^5$  Pa. The combination of the pressure used and drying process  
48 meant that the stack of disks held together sufficiently for subsequent handling.  
49  
50  
51  
52  
53  
54  
55  
56

#### (4) Electrophoretic impregnation and gravitational settling

Fig. 2b is a schematic diagram of the experimental arrangement used for the electrophoretic impregnation process. Initially, flat stainless steel plates were used as electrodes, Fig. 3a, placed vertically in the suspension 15 mm apart. The fiber preforms were attached to the anode since gas formed at the cathode that could have become trapped in the green compact. Two further electrode systems were devised following the initial results with the vertical electrodes, these being (i) vertical electrodes accommodating a rotating device for the anode, Fig. 3b, with speeds from 0 to 6 rpm and (ii) horizontal electrodes, Fig. 3c. The latter were also used without an electric field for comparative work involving the gravitational settling (GS) of particles. The authors are not aware of any previous work in terms of impregnating fiber preforms using simple gravitational settling; it was used simply to get a feel for how important the electrical field was.

For each impregnation a fabric disc measuring 48 mm diameter was laid on top of the appropriate anode and a polypropylene (PP) mask the same size as the electrode clamped over it using plastic grips. The PP cover had a 40 mm internal diameter opening cut in it to allow impregnation to occur into the preform; it should be noted that this design prevented any deposition of SiC powder in the outer 4 mm of the preform. Electrophoretic impregnations were carried out by applying a potential difference ranging from 50 to 100 V in constant voltage mode using slurries B and C. Each fabric disc was processed and the anode wiped clean of slurry before the next disc was attached on top of the previous, wet disc. The whole process was performed as fast as possible and the stack of ten powder impregnated discs was then allowed to dry overnight at room temperature. For all of the EPI-based processes, the final drying stage provided some strength to the stack of disks but they needed very careful handling.

For the gravitational settling (GS) process, the horizontal anode was used with no applied field. Each fabric disc was mounted on the anode as for the EPI process and held in place by the PP

cover. The slurry was stirred and, the moment the stirring stopped, the anode was plunged to the bottom of the beaker containing the suspension for a set period of time. The anode was then removed from the beaker and a fresh fabric disc placed in position on top of the wet one and the process repeated until a preform consisting of ten discs had been produced. Once again, the stack of discs produced needed very careful handling to prevent them delaminating.

#### (5) Combined process

Fabric discs were initially infiltrated with slurries B and C using the EPI and GS processes and then subsequently consolidated using the VB process as described previously. The use of the latter provided adequate strength to the stack for subsequent handling.

#### (6) Characterisation

Specimen diameters and thicknesses were measured using a vernier calliper gauge. The relative fiber volume,  $V_f$ , and relative powder volume,  $V_p$ , of the preforms (as a percentage of the total preform volume) were determined from the mass of the preform prior to powder impregnation,  $m_f$ , and its mass after powder impregnation,  $m_s$ , (from which the mass of powder impregnated,  $m_p$ , could be calculated) and the actual volume of the preforms,  $V_s$ , the latter being calculated from its geometry:

$$V_f = \frac{m_f}{V_s \rho_f} \times 100 \text{ (\%)} \quad (1)$$

$$V_p = \frac{(m_s - m_f)}{V_s \rho_{\text{SiC}}} = \frac{m_p}{V_s \rho_{\text{SiC}}} \times 100 \text{ (\%)} \quad (2)$$

where  $\rho_f$  is the density of NL-202 Nicalon fiber ( $2.55 \text{ g cm}^{-3}$ ) and  $\rho_{\text{SiC}}$  is the density of stoichiometric SiC ( $3.21 \text{ g cm}^{-3}$ ).

Assessment of the efficiency of the different processes was achieved by calculating the void reduction:

$$V.R. = \left(1 - \frac{100 - (V_f + V_p)}{100 - V_f}\right) \times 100 \quad (\%) \quad (3)$$

Comment [JB1]: Equation corrected (extra pair of brackets inserted).

Scanning electron microscopy was used to study both the powder distribution across the sample and the level of impregnation into the intratow and intertow porosity. The use of secondary and backscattered electron imaging allowed the powder additions to be differentiated with clarity from the fibers.

Dual energy X-ray absorptiometry (DEXA) also provided information on the powder distribution after impregnation. A Lunar DPX-L DEXA was calibrated for SiC materials<sup>11</sup> and photon attenuation maps acquired which, particularly when artificially coloured, provided a clear, qualitative representation of density variations across the diameter of the specimens.

Using Darcy's law for laminar viscous flow in porous materials<sup>37</sup>, the gas permeability of the samples,  $K$ , was calculated by plotting the ratio of the pressure difference across the sample thickness against the airflow. This provided a rough measure of the permeability of the preforms, with a view to ensuring that a subsequent CVI process would be capable of occurring. The pressure drop,  $\Delta P$ , across the preforms (thickness  $L$ ) was measured from the difference between the inlet and outlet pressure in a permeability rig similar to that described elsewhere<sup>38</sup>. The viscosity of the air was taken as  $\mu_{air} = 1.827 \times 10^{-5}$  Pa s.

### III Results & Discussion

As indicated above, the primary aim of the impregnation experiments was to reduce the intertow ~~porosity-pore sizes~~ of the preform, in order to shorten a subsequent chemical vapour infiltration process (not reported in this work), whilst ensuring that the preform has enough green strength

1  
2  
3  
4  
5  
6  
7  
8  
9  
10  
11 to allow handling and that the intratow porosity was accessible for infiltration. The distribution of  
12 the powder in the intertow and intratow porosity, as well as the uniformity of its distribution  
13 across the fiber preform, were therefore of key importance.  
14

15  
16  
17 Throughout the results, including Tables II – IV, the samples are identified by a code in which  
18 the first letter(s) is indicative of the impregnation system used; V for vacuum bagging, E for  
19 electrophoretic impregnation, G for gravitational settling, EV for combined electrophoretic  
20 impregnation and vacuum bagging and GV for combined gravitational settling and vacuum  
21 bagging.  
22  
23  
24  
25

#### 26 27 28 **(1) Vacuum bagging**

29  
30 The vacuum bagging results are shown in Table II and Fig. 4. As expected, it can be seen that  
31 the amount of powder impregnated into the preforms (indicated by the values of  $V_p$ ) was mainly  
32 influenced by the solids loading of the slurry, rather than the particle size. Repeatability of the  
33 results were confirmed with similar samples displaying  $V_p$  values (and hence V.R. and relative  
34 density values) ~~of  $\pm 4\%$  within  $\pm 1\%$  variation~~. SEM analysis revealed that compaction of the layers  
35 occurred with the intertow ~~porosity pores~~ being reduced to typically 50-100  $\mu\text{m}$  wide ~~(the~~  
36 ~~uncompacted intertow pores were up to  $\sim 500 \mu\text{m}$  wide)~~. When the solids loading was  $\geq 30 \text{ vol.}\%$   
37  
38  
39  
40  
41  
42 the particles systematically infiltrated these intertow voids leaving only a few, small regions  
43 unfilled, Fig. 5a. In contrast, when a 20% slurry was used very little intertow powder  
44 impregnation occurred, Fig. 5b, with just a little localised impregnation. For all solids contents,  
45  
46  
47  
48  
49  
50  
51  
52  
53  
54  
55  
56  
57  
58  
59  
60

When the degree of impregnation of powder in the intertow pores was substantial, cracks

1  
2  
3  
4  
5  
6  
7  
8  
9  
10  
11 appeared during the drying process in the intertow regions, the cracks usually being parallel to  
12 the fabric layers, Fig. 5c. It is believed that these were caused by the shrinkage of the powder  
13 matrix within the large intertow pores as a result of drying, whilst the fiber architecture prevented  
14 the preform as a whole from shrinking. The effect was less pronounced when a larger particle  
15 size was used.  
16  
17  
18

19  
20  
21 DEXA characterisation on the green preforms provided very clear, if qualitative, information on  
22 the powder distribution across the samples, Fig. 6a. When high solids content suspensions were  
23 used less uniformly impregnated samples resulted, presumably as a result of the higher viscosity  
24 of these suspensions, which made them more difficult to brush uniformly across the fabric discs.  
25  
26 Similarly, when the finer powders were used the particles may be seen to be mainly located  
27 around the edges of the preforms whilst the reverse was true for the larger particle sizes. This  
28 may be due to the applied pressure squeezing the finer powders outwards towards the edge of  
29 the preforms during the compaction stage. These results suggest that a more uniform  
30 distribution of the initial precursor suspension across the fabric discs and the use of intermediate  
31 particle sizes, in the range 5 – 8  $\mu\text{m}$ , are desirable to maximise the uniformity in the powder  
32 impregnation of the preforms.  
33  
34  
35  
36  
37  
38  
39  
40  
41

42 Whilst the gas permeability results in Table II showed relatively little variation as a function of  
43 particle size or solid loading for the samples measured, they do show that the introduction of  
44 powder reduced the permeability significantly, from  $16 \times 10^{-12} \text{ m}^2$  for a powderless preform<sup>11</sup> to  
45 values of  $1 - 2 \times 10^{-12} \text{ m}^2$ . This suggests strongly that the powder blocks a significant fraction of  
46 the gas paths necessary for CVI. Subsequent work<sup>389</sup>, however, demonstrated that all of the  
47 preforms could be successfully infiltrated by CVI.  
48  
49  
50  
51  
52

53  
54 Finally, it should be noted that whilst no mechanical test data was gathered for any of the  
55  
56

1  
2  
3  
4  
5  
6  
7  
8  
9  
10  
11 impregnated preforms produced in this work, those processed by VB were thinner, stronger,  
12 very handleable and less susceptible to delamination compared to the other methods. This is  
13 believed to result from the compression used under vacuum whilst the preform was still moist,  
14 the whole preform being strongly compacted.  
15  
16  
17

## 18 19 (2) Electrophoretic infiltration

20  
21 **Vertical electrode:** Due to settling of the powder in the suspension, it was not possible to  
22 achieve EPI successfully using vertical electrodes with powders coarser than 2.5  $\mu\text{m}$ ; the results  
23 obtained using the finer powders for suspension B are shown in Table III and Fig. 7. Irrespective  
24 of the particle sizes used, there was a clear trend as a function of the product of voltage and  
25 time, Fig. 7, with increased deposition being achieved at higher voltages and longer times as  
26 expected. However, for a given product of voltage  $\times$  time the 0.6  $\mu\text{m}$  particles resulted in greater  
27 powder deposition than the 2.5  $\mu\text{m}$  particles (provided all layers within the tow were  
28 impregnated), which in turn led to greater porosity reduction, Table III. In addition, the powder  
29 deposition rate decreased as processing time increased, compare for example, E/5/25-100/30  
30 and E/5/25-100/60 in Table III. This is also not surprising since the deposition rate is affected by  
31 the particle concentration in the suspension. This will decrease as deposition progresses,  
32 especially when the initial solids loading is low and the suspension is not stirred. Although the  
33 effect of stirring was briefly investigated, it was found that the gain in mass was reduced  
34 indicating that the movement of particles in the electric field was perturbed.  
35  
36  
37  
38  
39  
40  
41  
42  
43  
44  
45  
46  
47

48 SEM examination revealed that both sizes of powder deposited on the front surface of each  
49 fabric layer forming a continuous film covering the exposed surface, with very little SiC powder  
50 penetration within the fiber tows, Fig. 8a and 8b. As expected, the 0.6  $\mu\text{m}$  particles penetrated a  
51 little further than the 2.5  $\mu\text{m}$  particles, however higher voltages resulted in less penetration.  
52  
53  
54  
55  
56  
57  
58  
59  
60

1  
2  
3  
4  
5  
6  
7  
8  
9  
10  
11 Although this is perhaps counter-intuitive, higher voltages will have resulted in the particles  
12 accumulating on the fabric surface more rapidly, consequently blocking the paths into the  
13 intratow porosity. Nevertheless, the powders were deposited with a high density in the intertow  
14 porosity, Fig. 8c, leaving relatively few unimpregnated regions after stacking the fabric layers to  
15 form the preforms, Fig. 8a. Despite this, the impregnated preforms were very weak and suffered  
16 delamination very easily, preventing gas permeabilities being measured.

17  
18  
19  
20  
21  
22  
23 DEXA characterisation showed that the powder tended to form a 'crown' pattern around the  
24 centre, leaving the centre less impregnated than the periphery, Fig. 6b (the lack of deposition  
25 around the circumference arises from the presence of the polypropylene mask used to keep the  
26 fabric layer attached to the electrode). It is believed that this was caused by the lack of stirring  
27 during deposition resulting in sedimentation and hence preferential deposition at the bottom of  
28 each fabric layer attached to the electrode. Once randomly stacked up together, the 'crown'  
29 pattern was formed.

30  
31  
32  
33  
34  
35  
36  
37 **Rotating electrode:** Since stirring the slurry reduced mass deposition by disturbing the motion  
38 of the particles within the suspension, a rotating electrode approach was investigated to improve  
39 the uniformity of the powder distribution across the fabric area. Whilst very little variation in the  
40 mass of powder deposited was observed in the range 0 to 6 rpm, a rotation of 3 rpm was found  
41 to be the optimum speed based on the uniformity of the powder deposition. This electrode  
42 proved to be more tolerant of stirring of the suspension and very low stirring speeds were found  
43 to benefit the uniformity of deposition on the fabric surface without significantly affecting the  
44 amount of powder deposited.

45  
46  
47  
48  
49  
50  
51  
52  
53 **Horizontal electrode:** The horizontal electrode arrangement enabled larger SiC particles to be  
54 deposited, indeed they benefited the process by adding a degree of gravitational settling and so,



1  
2  
3  
4  
5  
6  
7  
8  
9  
10 as expected, the masses deposited were slightly more than for the vertical electrode, Fig. 9.  
11 They also resulted in less intratow penetration whilst continuing to achieve successful filling of  
12 the intertow porosity. The most even distributions across the fabric surface were observed to  
13 occur for deposition times of less than 90 s.  
14  
15  
16  
17

18  
19 When the horizontal electrode was used without the application of an electric field, i.e. pure  
20 gravitational settling (GS), the mass of powder deposited was approximately halved but the  
21 distribution of powder across the fabric surface was slightly more even and the intertow  
22 macrovoids were efficiently filled, irrespective of the slurry used. This is presumably because the  
23 slower deposition rate yielded a more uniform build up of powder.  
24  
25  
26  
27  
28

29  
30 Throughout the work using EPI, the ethanol-based slurry B took less time to dry, but resulted in  
31 a greater degree of cracking and delamination of the preforms than the aqueous-based slurry C,  
32 presumably because of the faster rate of solvent movement.  
33  
34  
35

### 36 37 **(3) Combined processes**

38 Table IV summarises the results obtained when powder was deposited on the fabric layers from  
39 slurry C by EPI, using the horizontal electrode arrangement and 50 V for 60 s, and then the  
40 resulting preforms were consolidated by VB. Very uniform powder deposition across the fabric  
41 layers was observed, Fig. 6c, with the intertow porosity densely filled but almost no penetration  
42 of the particles into the intratow porosity when the 6.7 and 10  $\mu\text{m}$  SiC particle sizes were used,  
43 Fig. 10. The major advantage observed for this technique was the ability to produce relatively  
44 strong and well compacted preforms from the VB stage of the process, with high densities as a  
45 result of the EPI process, but without the SiC particles filling the intratow voids when the coarser  
46 SiC particles were used. Despite the higher densities, the gas permeabilities were a factor of 3 –  
47 6 higher than for the VB route on its own supporting the view that the intratow gas channels, so  
48  
49  
50  
51  
52  
53  
54  
55  
56

1  
2  
3  
4  
5  
6  
7  
8  
9  
10 important for CVI, had not become blocked.  
11  
12

13  
14 Table IV also shows the results obtained when gravitational settling of the SiC particles was  
15 used to coat the fabric layers using the horizontal electrode but without any electric field and  
16 then the preforms were consolidated using the VB process. Once again, the powder distribution  
17 across the preform diameter was uniform, the intertow porosity was densely filled and the  
18 intratow porosity remained largely empty. Although the gas permeability was similar for the  
19 combined EPI/VB process for the aqueous slurry C, when the ethanol-based slurry B was used  
20 the value was approximately doubled to almost that of the unimpregnated preforms.  
21  
22  
23  
24  
25  
26

#### 27 28 **IV Conclusions**

29 Both the VB and EPI processes led to the impregnation of SiC fabric preforms with SiC powders,  
30 although the distribution of the powder was significantly different in the two cases, affecting both  
31 the strength and gas permeability of the final preforms. With the VB process, the SiC powder  
32 was forced into the intratow porosity and only filled the intertow porosity if the solids content of  
33 the suspension was sufficiently high; the opposite of what was required. In addition, the process  
34 relied on the manual brushing of the suspension onto the fabric disks; a process that led to a  
35 degree of variability despite attempts to control it. Much more uniform, controllable and  
36 reproducible deposition was achieved with the EPI process, with the intertow porosity being filled  
37 particularly densely but relatively little penetration of the particles into the intratow porosity,  
38 particularly when larger SiC particles were used. To avoid non-uniform distribution of the  
39 particles across the SiC fabric layers, a horizontal electrode arrangement was developed. This  
40 actually yielded slightly superior preforms when the electric field was turned off and gravity alone  
41 used to achieve deposition, although the time required obviously increased.  
42  
43  
44  
45  
46  
47  
48  
49  
50  
51  
52

53  
54 The main problem with the EPI process was that the resulting preforms were particularly weak  
55  
56

1  
2  
3  
4  
5  
6  
7  
8  
9  
10 and delaminated easily during handling. In contrast, the VB-formed preforms were relatively  
11 strong. The combination of EPI using a horizontal electrode, with or without the electric field  
12 switched on, followed by VB yielded strong preforms with a high degree of powder loading but  
13 which also retained a high level of gas permeability, a major requirement for the subsequent CVI  
14 stage.  
15  
16  
17  
18  
19

### 20 21 **Acknowledgements**

22 The authors would like to acknowledge funding by QinetiQ Ltd (formerly the Defence Evaluation  
23 Research Agency (DERA) of the UK).  
24  
25  
26  
27  
28  
29  
30  
31  
32  
33  
34  
35  
36  
37  
38  
39  
40  
41  
42  
43  
44  
45  
46  
47  
48  
49  
50  
51  
52  
53  
54  
55  
56  
57  
58  
59  
60

## References

1. T. M. Besmann, B. W. Sheldon, R. A. Lowden and D. P. Stinton, "Vapor-phase fabrication and properties of continuous-filament ceramic composites", *Science* **253** 1104-1109 (1991).
2. R. Naslain, "Design, preparation and properties of non-oxide CMCs for application in engines and nuclear reactors: an overview", *Comp. Sci. and Techn.* **64** 155-170 (2004).
3. D. Brewer, "HSR/EPM combustor materials development program", *Mater. Sci. Eng.* **A261** 284-291 (1999).
4. K. J. Probst., T. M. Besmann., D. P. Stinton, R. A. Lowden, T. J. Anderson and T.L. Starr, "Recent advances in forced-flow, thermal-gradient CVI for refractory composites", *Surfaces and Coatings Techn.* **120-121** 250-258 (1999).
5. B.W.Sheldon, "The control of gas phase kinetics to maximize densification during chemical vapour infiltration", *J. Mater. Res.* **5** [11] 2729-2736 (1990).
6. S. Bertrand., J. F. Lavaud, R. El Hadi, G. Vignoles and R. Pailler, "The thermal gradient-pulse flow CVI process: a new chemical vapour infiltration technique for the densification of fibre preforms", *J. Eur. Ceram. Soc.* **18** 857-870 (1998).
7. J.H. Kinney, T.M. Breunig, T.L. Starr, D. Haupt, M.C. Nichols, S.R. Stock, M.D. Butts and R.A. Saroyan, "X-ray tomographic study of chemical vapour infiltration processing of ceramic composites", *Science* **260** 789-791 (1993).
8. J.Y. Ofori and S.V. Sotirchos, "Dynamic convection-driven thermal gradient chemical vapour infiltration", *J. Mater. Res.* **11** [10] 2541-2555 (1996).
9. D. J. Skamser, J. J. Thomas, H.M. Jennings and D.L. Johnson, "Microwave heating of a changing material", *Ceram. Trans.* **59** 289-298 (1995).
10. A. Ortona, A. Donato, G. Filacchioni, U. De Angelis, A. La Barbera, C. A. Nannetti, B. Riccardi and J. Yeatman, "SiC-SiC<sub>f</sub> CMC manufacturing by hybrid CVI-PIP techniques:

- 1  
2  
3  
4  
5  
6  
7  
8  
9  
10 process optimisation", *Fusion Eng. and Design* **51-52** 159-163 (2000).
- 11  
12  
13 11. D. Jaglin, J. Binner, B. Vaidhyanathan, C. Prentice, R.A. Shatwell and D.G. Grant,  
14 "Microwave heated chemical vapour infiltration: Densification mechanism of SiC<sub>f</sub>/SiC  
15 Composites", *J. Am. Ceram. Soc.* **89** [9] 2710-2717 (2006).
- 16  
17  
18 12. R.J. Shinavski and R.J. Diefendorf, "CVI processing of thin C/HfB<sub>2</sub> composites", *Ceram.*  
19 *Eng. Sci. Proc.* **14** [9/10] 824-831 (1993).
- 20  
21  
22 13. M. Jones and T.L. Starr, "Enhancements to the Georgia Tech. chemical vapour infiltration  
23 process model for ceramic matrix composites", *Ceram. Eng. Sci. Proc.* **16** [5] 829-836  
24 (1995).
- 25  
26  
27 14. W.J. Lackey, S. Vaidyaraman, G.B. Freeman and P.K. Agrawal, "Technique for monitoring  
28 densification during chemical vapour infiltration", *J. Am. Ceram. Soc.* **78** [4] 1131-1133  
29 (1995).
- 30  
31  
32 15. T. Yano, K. Budiyo, K. Yoshida and T. Iseki, "Fabrication of silicon carbide fiber-  
33 reinforced silicon carbide composite by hot-pressing", *Fusion Eng. and Design* **41** 157-163  
34 (1998).
- 35  
36  
37 16. A. Sayano, C. Sutoh, S. Suyama, Y. Itoh and S. Nakagawa, "Development of a reaction-  
38 sintered silicon carbide matrix composite", *J. Nucl. Mater.* **271-272** 467-471 (1999).
- 39  
40  
41 17. J. J. Brennan, "Interfacial characterization of a slurry-cast melt-infiltrated SiC/SiC ceramic-  
42 matrix composite", *Acta Mater.* **48** 4619-4628 (2000).
- 43  
44  
45 18. D. Brewer, "HSR/EPM combustor materials development program", *Mater. Sci. Eng.* **A261**  
46 284291 (1999).
- 47  
48  
49 19. H. O. Davies and D. R. Petrak, "Ceramic matrix composites using polymer pyrolysis and  
50 liquid densification processing", *J. Nucl. Mater.* **219** 26-30 (1995).
- 51  
52  
53  
54  
55  
56  
57  
58  
59  
60

- 1  
2  
3  
4  
5  
6  
7  
8  
9  
10  
11 20. J. Gotoh, K. Tsugeki, A. Sakai and H. Nakayama, "Fabrication and mechanical properties of  
12 ceramic matrix composites by polymer impregnation and pyrolysis method", *Proc. 4<sup>th</sup> Japan*  
13 *Int. SAMPE Symp.* pp. 240-245 (1995).  
14  
15  
16 21. M.F. Gonon and S. Hampshire, "Comparison of two processes for manufacturing ceramic  
17 matrix composites from organometallic precursors", *J. Eur. Ceram. Soc.* **19** 285-291 (1999).  
18  
19 22. Y-W. Kim, J-S. Song, S-W. Park and J-G. Lee, "Nicalon-fibre-reinforced silicon-carbide  
20 composites via polymer solution infiltration and chemical vapour infiltration", *J. Mater. Sci.*  
21 **28** 3866-3868, (1993.)  
22  
23 23. S. Casadio, A. Donato, C.A. Nannetti, A. Ortona and M. Rescio, "Liquid infiltration and  
24 pyrolysis of SiC matrix composite materials", *Ceram. Trans.* **58** 193-198 (1995).  
25  
26 24. S. M. Dong, Y. Katoh, A. Kohyama, S. T. Schwab and L. L. Snead, "Microstructural  
27 evolution and mechanical performances of SiC/SiC composites by polymer  
28 impregnation/microwave pyrolysis (PIMP) process", *Ceram. Int.* **28** 899-905 (2002).  
29  
30 25. G. Ziegler, I. Ritcher and D. Suttor, "Fiber-reinforced composites with polymer-derived  
31 matrix: processing matrix formation and properties", *Composites: Part A* **30** 411-417 (1999).  
32  
33 26. G.R. Sherwin, "Non-autoclave processing of advanced composite repairs", *Int. J. of*  
34 *Adhesion & Adhesives* **19** 155-159 (1999).  
35  
36 27. G. Sala, "Advances in elastomeric tooling technology", *Materials & Design* **17** [1] 33-42  
37 (1996).  
38  
39 28. M.Z. Berbon, D.R. Dietrich, D.B. Marshall and D.P.H. Hasselman, "Transverse thermal  
40 conductivity of thin C/SiC composites fabricated by slurry infiltration and pyrolysis", *J. Am.*  
41 *Ceram. Soc.* **84** [10] 2229-2234 (2001).  
42  
43 29. A. Timms, W. Westby, C. Prentice, D. Jaglin, R. A. Shatwell and J. G. Binner, "Reducing  
44 chemical vapour infiltration time for ceramic matrix composites", *J. Microsc.*, **201-202** 316-  
45  
46  
47  
48  
49  
50  
51  
52  
53  
54  
55  
56  
57  
58  
59  
60

- 1  
2  
3  
4  
5  
6  
7  
8  
9  
10 323 (2001).  
11  
12  
13 30. P. Sarkar, S. Datta and P.S. Nicholson, "Functionally graded ceramic/ceramic and  
14 metal/ceramic composites by electrophoretic deposition", *Composites Part B* **28B** 49-56  
15 (1997).  
16  
17  
18 31. S.N. Heavens, "Electrophoretic deposition as a processing route for ceramics", *Advanced*  
19 *Ceramic Processing & Technology Vol. 1*, pp. 255-283, Ed. J.G.P. Binner, Noyes  
20 Publications (1990).  
21  
22  
23 32. A.R. Boccaccini, I. MacLaren and M.H. Lewis, "Electrophoretic deposition infiltration of 2-D  
24 woven SiC fibre mats with mixed sols of mullite composition", *J. Eur. Ceram. Soc.* **17** 1545-  
25 1550 (1997).  
26  
27  
28 33. A. Borner and R. Herbig, "ESA measurement for electrophoretic deposition of ceramic  
29 materials", *Colloids and Surfaces A: Physicochemical and Engineering Aspects* **159** 439-  
30 447 (1999).  
31  
32  
33 34. H.H. Streckert and J.D. Katz, "Microwave densification of electrophoretically infiltrated  
34 silicon carbide composite", *J. Mater. Sci.* **32** 6429-6433 (1997).  
35  
36  
37 35. S. Kooner, J.J. Campaniello S., Pickering and E. Bullock, "Fiber reinforced ceramic matrix  
38 composite fabrication by electrophoretic infiltration", *Ceram. Trans.* **58** 155-160 (1995).  
39  
40  
41 36. D. Jaglin, J. Binner, C. Prentice, R. Shatwell, L. Timms and W. Westby, "SiC<sub>f</sub>/SiC fabrication  
42 via vacuum bagging, electrophoretic infiltration and microwave enhanced CVI", 9<sup>th</sup> Eur.  
43 Conf. on Composite Materials (ECCM 9) proceedings CD, Institute of Materials, Minerals and  
44 Mining, UK (2000).  
45  
46  
47 37. A. P. Philipse, "Non-darcian airflow through ceramic foams", *J. Am. Ceram. Soc.*, **74** [4] 728-  
48 732 (1991).  
49  
50  
51  
52  
53  
54  
55  
56  
57  
58  
59  
60

- 1  
2  
3  
4  
5  
6  
7  
8  
9  
10  
11 38. T. L. Starr and N. Hablutzl, "Measurement of gas transport through fiber preforms and  
12 densified composites for chemical vapour infiltration," *J. Am. Ceram. Soc.* **81** [5] 1298–304  
13 (1998).  
14  
15  
16 39. J. Binner, B. Vaidhyanathan and D. Jaglin, "Microwave heated chemical vapour infiltration of  
17 SiC powder impregnated SiC fibre preforms", *Advances in Applied Ceramics: Structural,*  
18 *Functional and Bioceramics, In Press.*  
19  
20  
21  
22  
23  
24  
25  
26  
27  
28  
29  
30  
31  
32  
33  
34  
35  
36  
37  
38  
39  
40  
41  
42  
43  
44  
45  
46  
47  
48  
49  
50  
51  
52  
53  
54  
55  
56  
57  
58  
59  
60



## Captions

Fig. 1: SEM images of SiC<sub>f</sub>/SiC composites processed by CVI (a) low magnification showing large intertow voids and (b) high magnification showing fine intratow porosity. 72 x 72 dpi

Fig. 2: Schematic diagrams showing (a) the vacuum bagging equipment and (b) the electrophoretic impregnation system. 72 x 72 dpi

Fig. 3: Design variations for the anode used for EPI of SiC powder from suspension onto SiC fabric layers. 72 x 72 dpi

Fig. 4a: Reduction in porosity observed in the VB preforms as a function of the solids loading in the SiC slurries. 72 x 72 dpi

Fig. 4b: Reduction in porosity observed in the VB preforms as a function of the particle size in the SiC slurries. 72 x 72 dpi

Fig. 5: SEM cross sectional micrographs of preforms prepared by VB at two different magnifications (a) and (c) V/30/6, (b) and (d) V/20/6. 72 x 72 dpi

Fig. 6: Colour enhanced ERA-DEXA scans for samples prepared by a) VB, b) EPI using the vertical electrode and c) combined VB and EPI using the horizontal electrode. 72 x 72 dpi

Fig. 7: Reduction in porosity versus (voltage x time) applied during the EPI process using the vertical electrode. 72 x 72 dpi

1  
2  
3  
4  
5  
6  
7  
8  
9  
10  
11 Fig. 8: Low and high magnification SEM images of cross sections of preforms formed by EPI (a)  
12 and (b) E/5/6-50/90† and (c) E/5/6-100/45. 72 x 72 dpi  
13  
14

15  
16 Fig. 9: Reduction in porosity versus deposition time for EPI using the vertical (V) and horizontal  
17 (H) electrodes and different SiC particle sizes. 72 x 72 dpi  
18  
19

20  
21 Fig. 10: Low and high magnification SEM images of cross sections of preforms formed by  
22 combined VB and EPI (a) and (b) EV/5/25-50/60; (c) and (d) EV/5/67-50/60 and (e) and (f)  
23 EV/5/100-50/60. 72 x 72 dpi  
24  
25  
26  
27  
28  
29  
30

31 Table I: Mean particle size and source of SiC particles used.  
32  
33

34 Table II: Impregnation results achieved by the VB process.  
35  
36  
37

38 Table III: Impregnation results achieved by the EPI process.  
39  
40

41 Table IV: Impregnation results achieved by the combined horizontal EPI and VB processes and  
42 the combined horizontal GS and VB processes.  
43  
44  
45  
46  
47  
48  
49  
50  
51  
52  
53  
54  
55  
56  
57  
58  
59  
60

Table I: Mean particle size and source of SiC particles used.

| Mean particle size / $\mu\text{m}$ | Source  |
|------------------------------------|---|
| 0.6                                | UF15, HC Starck, Goslar, Germany  |
| 2.5                                | ESK1500F, ESK, Kempton, Germany   |
| 6.7                                | Reliable Techniques, Newcastle-under-Lyme, UK                                 |
| 10.0                               | Carborex BW Micro F 600 PV, Washington Mills Electro Minerals, Manchester, UK |
| 12.8                               | Silkaride CS F1200, Washington Mills Electro Minerals, Manchester, UK         |

Table II: Impregnation results achieved by the VB process.

| Sample   | Slurry type | Solid loading / % | Particle size / $\mu\text{m}$ | $V_f$ / % | $V_p$ / % | V.R. / % | Relative density / % | Gas permeability <sup>#</sup> / $10^{-12} \text{ m}^2$ |
|----------|-------------|-------------------|-------------------------------|-----------|-----------|----------|----------------------|--|
| V/20/6   | A           | 20                | 0.6                           | 25        | 9         | 12       | 34                   | *  |
| V/20/25  | A           | 20                | 2.5                           | 23        | 6         | 10       | 29                   | *  |
| V/20/128 | A           | 20                | 12.8                          | 21        | 8         | 11       | 29                   | *  |
| V/30/6   | A           | 30                | 0.6                           | 35        | 15        | 23       | 50                   | *  |
| V/30/100 | A           | 30                | 10.0                          | 14        | 15        | 17       | 29                   | 1.3  |
| V/35/6   | A           | 35                | 0.6                           | 21        | 18        | 23       | 39                   | 2.0  |
| V/35/25  | A           | 35                | 2.5                           | 19        | 16        | 28       | 35                   | 1.9  |
| V/35/67  | A           | 35                | 6.7                           | 16        | 19        | 23       | 35                   | 1.8  |
| V/35/100 | A           | 35                | 10.0                          | 18        | 21        | 26       | 39                   | 1.1  |
| V/40/100 | A           | 40                | 10.0                          | 16        | 21        | 25       | 37                   | 1.0  |

<sup>#</sup> $16 \times 10^{-12} \text{ m}^2$  for a powderless preform

\*Technique not available at the time

Table III: Impregnation results achieved by the EPI process.

| Sample                   | Slurry type | Solid loading / % | Particle size / $\mu\text{m}$ | Electrode type    | Voltage / V | Time / s  | $V_f$ / % | $V_p$ / % | Void reduction V.R. / % | Relative density / % |
|--------------------------|-------------|-------------------|-------------------------------|-------------------|-------------|-----------|-----------|-----------|-------------------------|----------------------|
| E/5/6-50/45 <sup>†</sup> | B           | 5                 | 0.6                           | Vertical          | 50          | 45        | 21        | 7         | 9                       | 28                   |
| E/5/6-50/60              | B           | 5                 | 0.6                           | Vertical          | 50          | 60        | 17        | 15        | 18                      | 32                   |
| E/5/6-50/90              | B           | 5                 | 0.6                           | Vertical          | 50          | 90        | 16        | 18        | 21                      | 34                   |
| E/5/6-50/90 <sup>†</sup> | B           | 5                 | 0.6                           | Vertical          | 50          | 90        | 22        | 12        | 15                      | 34                   |
| E/5/6-100/45             | B           | 5                 | 0.6                           | Vertical          | 100         | 45        | 20        | 19        | 24                      | 39                   |
| E/5/25-50/60             | B           | 5                 | 2.5                           | Vertical          | 50          | 60        | 20        | 11        | 14                      | 31                   |
| E/5/25-100/30            | B           | 5                 | 2.5                           | Vertical          | 100         | 30        | 22        | 13        | 17                      | 35                   |
| E/5/25-100/60            | B           | 5                 | 2.5                           | Vertical          | 100         | 60        | 19        | 21        | 26                      | 40                   |
| E/10/25-50/60            | B           | 10                | 2.5                           | Vertical          | 50          | 60        | 18        | 26        | 32                      | 44                   |
| <u>E/5/25-50/60</u>      | <u>B</u>    | <u>5</u>          | <u>2.5</u>                    | <u>Horizontal</u> | <u>50</u>   | <u>60</u> | <u>18</u> | <u>12</u> | <u>15</u>               | <u>30</u>            |

† Alternate layers impregnated

Table IV: Impregnation results achieved by the combined horizontal EPI and VB processes and the combined horizontal GS and VB processes.

| Sample         | Slurry type | Solid loading / % | Particle size / $\mu\text{m}$ | $V_f$ / % | $V_p$ / % | Void reduction V.R. / % | Relative density / % | Gas permeability / $10^{-12} \text{ m}^2$ |
|----------------|-------------|-------------------|-------------------------------|-----------|-----------|-------------------------|----------------------|---|
| EV/5/25-50/60  | C           | 5                 | 2.5                           | 18        | 17        | 21                      | 35                   | 6.9                                       |
| EV/5/67-50/60  | C           | 5                 | 6.7                           | 21        | 18        | 23                      | 39                   | 6.8                                       |
| EV/5/100-50/60 | C           | 5                 | 10                            | 21        | 19        | 24                      | 40                   | 6.3                                       |
| GV/5/67-B      | B           | 5                 | 6.7                           | 17        | 19        | 23                      | 36                   | 12.8                                      |
| GV/5/67-C      | C           | 5                 | 6.7                           | 19        | 22        | 27                      | 41                   | 6.8                                       |
| GV/5/100-B     | B           | 5                 | 10                            | 21        | 20        | 25                      | 41                   | 10.6                                      |
| GV/5/100-C     | C           | 5                 | 10                            | 20        | 20        | 25                      | 40                   | 6.0                                       |

## Use of Electrophoretic Impregnation and Vacuum Bagging to Impregnate SiC powder into SiC Fiber Preforms

Jon Binner<sup>\*</sup>, Bala Vaidhyanathan, David Jaglin and Sarah Needham<sup>†</sup>

Department of Materials, Loughborough University, Loughborough, Leicestershire LE11 3TU, United Kingdom

### Abstract

Techniques based on vacuum bagging (VB) and electrophoretic impregnation (EPI) have been investigated for the impregnation of SiC powder into layered Nicalon SiC fabric preforms. The aim was to produce pre-impregnated samples for subsequent chemical vapour infiltration (CVI) with reduced intertow porosity that arises from the construction of the fabric layers whilst leaving unblocked the intratow porosity that is so indispensable for a successful infiltration. Since the goal was simply to learn about the ability to impregnate the samples, no interphase coating was applied to the fibers as would normally be used when producing SiC<sub>f</sub>-SiC composites. Whilst the VB process generally yielded much stronger preforms, depending on the pressure used and the powder particle size, it resulted in powder becoming located in the intratow rather than the intertow porosity. In contrast, provided an appropriate electrode arrangement was used, EPI offered the potential for a more controlled impregnation process with the powder primarily found in the intertow porosity; however, the preforms were very weak and delaminated easily. The combination of the two processes resulted in a very successful approach, with greater uniformity of particle infiltration and higher green strengths, whilst largely avoiding impregnating the intratow porosity.

---

<sup>\*</sup> J.binner@Lboro.ac.uk

<sup>†</sup> Now with Rolls Royce plc., UK

## I Introduction

SiC<sub>f</sub>/SiC composites are very promising materials for high temperature structural applications because of their good thermal stability and excellent mechanical properties. Of the various techniques used to produce fiber reinforced ceramic matrix composites, chemical vapour infiltration (CVI) has received considerable attention<sup>1-2</sup>. Combining isothermal or temperature gradient, isobaric or pressure gradient features, as well as the use of pulsing, CVI results in composites still containing 10 - 20% residual porosity<sup>3-6</sup> however. This is mainly due to two reasons: (i) when the minimum percolation threshold for transport through the pore structure is reached, infiltration becomes more and more difficult as the pore size decreases resulting in deposition occurring on the outside of the fiber network, and (ii) when the composite reaches a fractional density of ~70% the surface area becomes dominated by the macropores; these can take too long to infiltrate from a commercial viewpoint. It is the last 30% of densification that is financially costly because the infiltration time becomes extended (to days and even weeks in some cases) during this phase<sup>7</sup> and to produce fiber-reinforced ceramic matrix composites (FRCMCs) by any form of CVI at a commercially acceptable cost, the processing time must be kept short<sup>8</sup>.

As implied above, the porosity itself can be divided into two main types; fine intratow and much larger intertow porosity. In fibrous preforms densified up to 82% of theoretical<sup>9</sup>, the lamination of the plies combined with the weave design can result in intertow pores being as large as 0.3 to 0.6 mm in width and tens of millimetres long. There is also the problem of the packing of the fabric layer in the Z-direction<sup>10</sup>. Fig. 1a<sup>11</sup> provides an illustration of this type of porosity, which is the most harmful type of defect for mechanical properties as well as providing a path for corrosive agents. When present, these pores are very difficult to eliminate in fiber preforms produced from the lay-up of fiber sheets. In contrast, intratow pores are typically <15 μm in diameter and are formed when the matrix deposition on the individual fibers traps small pores,

1  
2  
3  
4  
5  
6 Fig. 1b. Whilst some will probably always be residual after CVI-based processes, they are not  
7  
8 considered to be particularly detrimental to the overall strength of the composite due to their  
9  
10 small size<sup>9</sup>. Nevertheless, the elimination of this porosity by the use of the right infiltration  
11  
12 conditions would also undoubtedly be desirable – provided it can be achieved without a  
13  
14 significant increase in processing time and hence costs.  
15  
16

17  
18  
19 Two-stage CVI processes have therefore been investigated where, under the right conditions,  
20  
21 the initial stage sees the efficient filling of the finer, intratow porosity and the second stage seeks  
22  
23 to fill as much of the coarser, intertow pores as possible within the economic limitations of the  
24  
25 process<sup>12-13</sup>. For example, using marker layers, Lackey *et al.*<sup>14</sup> found that when using forced-flow  
26  
27 CVI, intratow infiltration could be virtually complete within the first 2 h, although filling the intertow  
28  
29 porosity took considerably longer. One potential problem with this approach is that some  
30  
31 intertow porosity can become trapped in the structure when the intratow porosity becomes filled.  
32  
33

34  
35  
36 Although not the focus of this paper, many other techniques are available for the fabrication of  
37  
38 FRCMCs as well as CVI. For example, hot-pressing techniques have been used<sup>15</sup> in which the  
39  
40 stacked green body was hot-pressed at up to 2023 K with a matrix consisting of  $\beta$ -SiC powder  
41  
42 and sintering aids. Unfortunately, the composite displayed brittle behaviour even though Hi-  
43  
44 Nicalon fibers were used. An approach based on slurry-cast melt infiltration with reaction-  
45  
46 sintering<sup>16-18</sup> used a slurry consisting of SiC powder or a mixture of SiC powder and carbon  
47  
48 powder in water that was impregnated into the SiC fiber preform. The green composite was then  
49  
50 reaction sintered at 1720 K with melted silicon to obtain a rich SiC matrix. Disadvantages lay in  
51  
52 the need for a designed mould and residual silicon metal as high as 15-20 vol.%, despite the low  
53  
54 porosity achieved.  
55  
56

57  
58  
59 An alternative approach can be based on the pre-impregnation of the macropores by a process  
60

1  
2  
3  
4  
5  
6 other than CVI and polymer impregnation and pyrolysis (PIP) processes are very common and  
7 effective manufacturing techniques for high performance SiC<sub>f</sub>/SiC composites<sup>19-24</sup>. Six or more  
8 cycles of impregnations, followed by the pyrolysis, are typically required to achieve densities of  
9 80-85%. An important aspect of the process is that the matrix development affects the  
10 mechanical properties by inducing residual stresses due to shrinkage of the matrix during  
11 pyrolysis and also the anisotropy of the thermal expansion coefficient between the fibers and  
12 matrix<sup>25</sup>.  
13  
14  
15  
16  
17  
18  
19

20  
21  
22  
23 The introduction of powder into the PIP was investigated by Gonon and Hampshire<sup>21</sup> who used  
24 polysilazane as precursor with the addition of Si<sub>3</sub>N<sub>4</sub> powder into SiC fiber preforms; 7 to 8 cycles  
25 of precursor impregnation and pyrolysis were required to reduce the porosity to approximately  
26 15%, but the presence of powder did not allow good cross-linking of the precursor and resulted  
27 in lower mechanical properties than the composite with the polymer alone, a result confirmed by  
28 Casadio<sup>23</sup>. Gotoh *et al.*<sup>20</sup> also pointed out that optimisation of the mechanical properties relies on  
29 the right volume of fiber and sintering aids. Fast heating techniques such as microwaves can be  
30 applied during the pyrolysis stage, providing time and energy savings since suitably high  
31 temperatures can be induced in a matter of minutes. Dong and co-authors<sup>24</sup> used this particular  
32 technique but required 8 cycles of impregnation to achieve a final density of 78%.  
33  
34  
35  
36  
37  
38  
39  
40  
41  
42  
43  
44  
45

46 Combining PIP with CVI allowed Kim *et al.*<sup>22</sup> to achieve an initial preform density of up to 70%  
47 after PIP, the subsequent isobaric, isothermal CVI step yielding a composite density of 82%.  
48 Ortona *et al.*<sup>10</sup> found that an initial CVI stage can prevent the swelling of the preform during the  
49 PIP stages.  
50  
51  
52  
53  
54  
55

56 Two simple and rapid processes that have been shown to lead to a successful pre-impregnation  
57 in other, non-SiC fiber-based systems are vacuum bagging (VB) and electrophoretic  
58  
59  
60



1  
2  
3  
4  
5  
6 impregnation (EPI). VB is a relatively simple process that was developed by Rolls Royce in the  
7  
8 1980s for the preparation and/or repair of polymer matrix carbon fiber composites in the  
9  
10 aerospace industry<sup>26-28</sup>. This technique has subsequently been modified for the impregnation of  
11  
12 ceramic powders between tows and layers of fiber-based fabrics in order to reduce the porosity  
13  
14 and improve the green strength<sup>29</sup>. The fabric layers are individually coated with ceramic slurry  
15  
16 and stacked, prior to being dried and consolidated under vacuum. Process parameters are  
17  
18 mainly associated with the preparation of the slurry, which controls the particle size being used  
19  
20 and the amount of powder to be impregnated, and the pressure involved during vacuum  
21  
22 bagging.  
23  
24  
25

26  
27 EPI is directly related the electrophoretic deposition process (EPD) wherein charged particles  
28  
29 are deposited on an electrode surface via their migration under the action of an electrical field<sup>30</sup>.  
30  
31 In the EPI process, a fiber preform is impregnated via the deposition of particles from a slurry  
32  
33 onto individual cloth layers prior to assembly into the preform. The movement of ceramic  
34  
35 particles in a suspension within an electric field is governed mainly by factors such as the field  
36  
37 strength<sup>31</sup>, the pH of the suspension and its ionic strength<sup>32</sup>. The amount of polyelectrolyte  
38  
39 addition also influences the rate of deposition and the homogeneity of the deposited material<sup>33</sup>.  
40  
41 Green composite microstructures with good infiltration uniformity and few macro defects have  
42  
43 been obtained by this technique<sup>34-35</sup> and previous work with a SiC<sub>i</sub>/SiC system resulted an  
44  
45 increase in density from 20 vol.% (the initial fiber preform density) to over 40 vol.% in only 20  
46  
47 minutes<sup>36</sup>.  
48  
49  
50

51  
52 In the present work, a methodical examination of the use of stand-alone VB and EPI techniques  
53  
54 as well as their combination with a number of geometrical modifications has been undertaken  
55  
56 with a view to producing SiC powder-loaded SiC fiber preforms that are suitable for subsequent  
57  
58 infiltration with a SiC matrix using CVI. The goal was to fill the larger intertow pores, so reducing  
59  
60

1  
2  
3  
4  
5  
6 the time that would be needed during a subsequent CVI stage, whilst avoiding the introduction of  
7  
8 powder particles within the tows themselves. The particles can cause abrasion during use and  
9  
10 damage the tows. In addition, it was desired to produce impregnated fiber preforms that were  
11  
12 mechanically robust and capable of being handled prior to and during the CVI stage.  
13  
14

## 15 16 17 **II Experimental procedure**

### 18 19 **(1) Materials**

20 The preforms were made from NL-202 SiC fibers (Nippon Carbon, Tokyo, Japan) woven (by  
21  
22 Sigmalex Ltd., UK) into a 2D plain weave NP1616 pattern. Forty eight mm circular discs were  
23  
24 cut from the cloth using a metal template and ceramic scissors. The sizing agent was removed  
25  
26 by heating the fiber discs in a furnace at 600°C for 2 h. Note, no attempt was made in this work  
27  
28 to apply an interphase coating to the fibers prior to undertaking the impregnation with powder  
29  
30 particles. This was because it was not believed that such a coating would materially affect the  
31  
32 identification of the best choice of impregnation process, which was the goal of this work. For the  
33  
34 impregnation experiments themselves, five SiC powders with mean particle sizes of  
35  
36 approximately 0.6, 2.5, 6.7, 10.0 and 12.8  $\mu\text{m}$  were used; their details are provided in table 1.  
37  
38  
39  
40  
41

### 42 43 **(2) SiC powder slurry preparation**

44 Three types of slurries were prepared. Slurry A was used during the impregnation of preforms by  
45  
46 vacuum bagging (VB), whilst slurries B and C were used for electrophoretic impregnation (EPI)  
47  
48 and gravitational settling (GS).  
49

50  
51 **Slurry A:** Aqueous slurries containing solids loadings between 20 and 40 vol.% were prepared  
52  
53 for all five of the SiC powders. The powders were dispersed using 1 to 1.5 wt.% of Glascol K11  
54  
55 (Ciba Speciality Chemicals, Bradford, UK) and the pH was fixed at  $9.0 \pm 0.2$  via the addition of  
56  
57 ammonia solution. To eliminate powder agglomerates, the slurries were ball-milled in airtight  
58  
59  
60

1  
2  
3  
4  
5  
6 polyethylene bottles using zirconia media for 24 h, the viscosity being regularly monitored. Note  
7  
8 that, although slurries with a solid loading higher than 45 vol.%, were prepared, problems were  
9  
10 experienced with subsequent wetting of the fiber fabric and hence these slurries were discarded.  
11

12  
13 **Slurry B:** Ethanol-based slurries containing solids loadings of 5 and 10 vol.% were prepared for  
14  
15 four of the SiC powders, the powders being dispersed using 0.5 vol.% of triethylamine (Ciba  
16  
17 Speciality Chemicals, Bradford, UK); the pH was  $9.0 \pm 0.2$ . The  $12.8 \mu\text{m}$  SiC powder was not  
18  
19 used as it was found that particle migration was difficult to achieve at the voltages used. To  
20  
21 remove powder agglomerates, during preparation the slurries were exposed to ultrasonic energy  
22  
23 at 23 kHz (Soniprep 150 Ultrasonicator, MSE Scientific Instruments, Manchester, UK) for a  
24  
25 minimum of 60 s together with mechanical agitation using a magnetic stirrer.  
26  
27

28  
29 **Slurry C:** An identical preparation route as for slurry B was used to prepare aqueous  
30  
31 suspensions containing 5 vol.% of SiC powders for all five of the SiC powders, again with the  
32  
33 addition of  $\sim 0.5$  vol.% of triethylamine. The pH was again  $9.0 \pm 0.2$ . Ultrasonic energy and  
34  
35 mechanical agitation was again used, as described for slurry B.  
36  
37

### 38 39 (3) Vacuum bagging

40  
41 A small amount of slurry A was applied to the discs of SiC fabric using a nylon brush. Since the  
42  
43 impregnation of the powder was performed manually, the VB technique potentially lacked  
44  
45 repeatability with respect to the amount of powder deposited on each fabric layer. To minimise  
46  
47 this problem each layer was weighed after brushing to ensure that a consistent amount had  
48  
49 been deposited. Ten discs were then stacked and the layers compressed using a roller. Each  
50  
51 preform was placed in the vacuum bagging equipment (Townsend & Mercer Ltd., Croydon, UK),  
52  
53 Fig. 2a, and dried overnight at temperatures ranging from 20 to  $60^\circ\text{C}$ , a rotary pump being used  
54  
55 to apply a vacuum of  $\sim 0.5 \times 10^5$  Pa. The combination of the pressure used and drying process  
56  
57 meant that the stack of disks held together sufficiently for subsequent handling.  
58  
59  
60

#### (4) Electrophoretic impregnation and gravitational settling

Fig. 2b is a schematic diagram of the experimental arrangement used for the electrophoretic impregnation process. Initially, flat stainless steel plates were used as electrodes, Fig. 3a, placed vertically in the suspension 15 mm apart. The fiber preforms were attached to the anode since gas formed at the cathode that could have become trapped in the green compact. Two further electrode systems were devised following the initial results with the vertical electrodes, these being (i) vertical electrodes accommodating a rotating device for the anode, Fig. 3b, with speeds from 0 to 6 rpm and (ii) horizontal electrodes, Fig. 3c. The latter were also used without an electric field for comparative work involving the gravitational settling (GS) of particles. The authors are not aware of any previous work in terms of impregnating fiber preforms using simple gravitational settling; it was used simply to get a feel for how important the electrical field was.

For each impregnation a fabric disc measuring 48 mm diameter was laid on top of the appropriate anode and a polypropylene (PP) mask the same size as the electrode clamped over it using plastic grips. The PP cover had a 40 mm internal diameter opening cut in it to allow impregnation to occur into the preform; it should be noted that this design prevented any deposition of SiC powder in the outer 4 mm of the preform. Electrophoretic impregnations were carried out by applying a potential difference ranging from 50 to 100 V in constant voltage mode using slurries B and C. Each fabric disc was processed and the anode wiped clean of slurry before the next disc was attached on top of the previous, wet disc. The whole process was performed as fast as possible and the stack of ten powder impregnated discs was then allowed to dry overnight at room temperature. For all of the EPI-based processes, the final drying stage provided some strength to the stack of disks but they needed very careful handling.

For the gravitational settling (GS) process, the horizontal anode was used with no applied field. Each fabric disc was mounted on the anode as for the EPI process and held in place by the PP

cover. The slurry was stirred and, the moment the stirring stopped, the anode was plunged to the bottom of the beaker containing the suspension for a set period of time. The anode was then removed from the beaker and a fresh fabric disc placed in position on top of the wet one and the process repeated until a preform consisting of ten discs had been produced. Once again, the stack of discs produced needed very careful handling to prevent them delaminating.

### (5) Combined process

Fabric discs were initially infiltrated with slurries B and C using the EPI and GS processes and then subsequently consolidated using the VB process as described previously. The use of the latter provided adequate strength to the stack for subsequent handling.

### (6) Characterisation

Specimen diameters and thicknesses were measured using a vernier calliper gauge. The relative fiber volume,  $V_f$ , and relative powder volume,  $V_p$ , of the preforms (as a percentage of the total preform volume) were determined from the mass of the preform prior to powder impregnation,  $m_f$ , and its mass after powder impregnation,  $m_s$ , (from which the mass of powder impregnated,  $m_p$ , could be calculated) and the actual volume of the preforms,  $V_s$ , the latter being calculated from its geometry:

$$V_f = \frac{m_f}{V_s \rho_f} \times 100 (\%) \quad (1)$$

$$V_p = \frac{(m_s - m_f)}{V_s \rho_{SiC}} = \frac{m_p}{V_s \rho_{SiC}} \times 100 (\%) \quad (2)$$

where  $\rho_f$  is the density of NL-202 Nicalon fiber ( $2.55 \text{ g cm}^{-3}$ ) and  $\rho_{SiC}$  is the density of stoichiometric SiC ( $3.21 \text{ g cm}^{-3}$ ).

1  
2  
3  
4  
5  
6 Assessment of the efficiency of the different processes was achieved by calculating the void  
7  
8 reduction:

$$V.R. = \left(1 - \frac{100 - (V_f + V_p)}{100 - V_f}\right) \times 100 \quad (\%) \quad (3)$$

9  
10  
11  
12  
13  
14 Scanning electron microscopy was used to study both the powder distribution across the sample  
15  
16 and the level of impregnation into the intratow and intertow porosity. The use of secondary and  
17  
18 backscattered electron imaging allowed the powder additions to be differentiated with clarity  
19  
20 from the fibers.  
21

22  
23  
24  
25 Dual energy X-ray absorptiometry (DEXA) also provided information on the powder distribution  
26  
27 after impregnation. A Lunar DPX-L DEXA was calibrated for SiC materials<sup>11</sup> and photon  
28  
29 attenuation maps acquired which, particularly when artificially coloured, provided a clear,  
30  
31 qualitative representation of density variations across the diameter of the specimens.  
32

33  
34  
35 Using Darcy's law for laminar viscous flow in porous materials<sup>37</sup>, the gas permeability of the  
36  
37 samples,  $K$ , was calculated by plotting the ratio of the pressure difference across the sample  
38  
39 thickness against the airflow. This provided a rough measure of the permeability of the preforms,  
40  
41 with a view to ensuring that a subsequent CVI process would be capable of occurring. The  
42  
43 pressure drop,  $\Delta P$ , across the preforms (thickness  $L$ ) was measured from the difference  
44  
45 between the inlet and outlet pressure in a permeability rig similar to that described elsewhere<sup>38</sup>.  
46  
47

48 The viscosity of the air was taken as  $\mu_{air} = 1.827 \times 10^{-5}$  Pa s.  
49

### 50 51 52 53 **III Results & Discussion**

54  
55 As indicated above, the primary aim of the impregnation experiments was to reduce the intertow  
56  
57 pore sizes of the preform, in order to shorten a subsequent chemical vapour infiltration process  
58  
59 (not reported in this work), whilst ensuring that the preform has enough green strength to allow  
60

1  
2  
3  
4  
5  
6 handling and that the intratow porosity was accessible for infiltration. The distribution of the  
7  
8 powder in the intertow and intratow porosity, as well as the uniformity of its distribution across  
9  
10 the fiber preform, were therefore of key importance.  
11

12  
13  
14 Throughout the results, including Tables II – IV, the samples are identified by a code in which  
15  
16 the first letter(s) is indicative of the impregnation system used; V for vacuum bagging, E for  
17  
18 electrophoretic impregnation, G for gravitational settling, EV for combined electrophoretic  
19  
20 impregnation and vacuum bagging and GV for combined gravitational settling and vacuum  
21  
22 bagging.  
23  
24

### 25 26 27 **(1) Vacuum bagging**

28  
29 The vacuum bagging results are shown in Table II and Fig. 4. As expected, it can be seen that  
30  
31 the amount of powder impregnated into the preforms (indicated by the values of  $V_p$ ) was mainly  
32  
33 influenced by the solids loading of the slurry, rather than the particle size. Repeatability of the  
34  
35 results were confirmed with similar samples displaying  $V_p$  values (and hence V.R. and relative  
36  
37 density values) within  $\pm 1\%$  variation. SEM analysis revealed that compaction of the layers  
38  
39 occurred with the intertow pores being reduced to typically 50-100  $\mu\text{m}$  wide (the uncompact  
40  
41 intertow pores were up to  $\sim 500 \mu\text{m}$  wide). When the solids loading was  $\geq 30 \text{ vol.}\%$  the particles  
42  
43 systematically infiltrated these intertow voids leaving only a few, small regions unfilled, Fig. 5a.  
44  
45 In contrast, when a 20% slurry was used very little intertow powder impregnation occurred,  
46  
47 Fig. 5b, with just a little localised impregnation. For all solids contents, impregnation of the tows  
48  
49 occurred for the 0.6 and 2.5  $\mu\text{m}$  particle sizes as the pressure and vacuum applied during  
50  
51 vacuum bagging forced powder into the intratow voids, Figs. 5c and 5d.  
52  
53  
54  
55

56  
57 When the degree of impregnation of powder in the intertow pores was substantial, cracks  
58  
59 appeared during the drying process in the intertow regions, the cracks usually being parallel to  
60

1  
2  
3  
4  
5  
6 the fabric layers, Fig. 5c. It is believed that these were caused by the shrinkage of the powder  
7 matrix within the large intertow pores as a result of drying, whilst the fiber architecture prevented  
8 the preform as a whole from shrinking. The effect was less pronounced when a larger particle  
9 size was used.  
10  
11  
12  
13

14  
15  
16 DEXA characterisation on the green preforms provided very clear, if qualitative, information on  
17 the powder distribution across the samples, Fig. 6a. When high solids content suspensions were  
18 used less uniformly impregnated samples resulted, presumably as a result of the higher viscosity  
19 of these suspensions, which made them more difficult to brush uniformly across the fabric discs.  
20 Similarly, when the finer powders were used the particles may be seen to be mainly located  
21 around the edges of the preforms whilst the reverse was true for the larger particle sizes. This  
22 may be due to the applied pressure squeezing the finer powders outwards towards the edge of  
23 the preforms during the compaction stage. These results suggest that a more uniform  
24 distribution of the initial precursor suspension across the fabric discs and the use of intermediate  
25 particle sizes, in the range 5 – 8  $\mu\text{m}$ , are desirable to maximise the uniformity in the powder  
26 impregnation of the preforms.  
27  
28  
29  
30  
31  
32  
33  
34  
35  
36  
37  
38  
39  
40  
41

42 Whilst the gas permeability results in Table II showed relatively little variation as a function of  
43 particle size or solid loading for the samples measured, they do show that the introduction of  
44 powder reduced the permeability significantly, from  $16 \times 10^{-12} \text{ m}^2$  for a powderless preform<sup>11</sup> to  
45 values of  $1 - 2 \times 10^{-12} \text{ m}^2$ . This suggests strongly that the powder blocks a significant fraction of  
46 the gas paths necessary for CVI. Subsequent work<sup>39</sup>, however, demonstrated that all of the  
47 preforms could be successfully infiltrated by CVI.  
48  
49  
50  
51  
52  
53  
54  
55

56 Finally, it should be noted that whilst no mechanical test data was gathered for any of the  
57 impregnated preforms produced in this work, those processed by VB were thinner, stronger,  
58  
59  
60



1  
2  
3  
4  
5  
6 very handleable and less susceptible to delamination compared to the other methods. This is  
7  
8 believed to result from the compression used under vacuum whilst the preform was still moist,  
9  
10 the whole preform being strongly compacted.  
11

## 12 13 14 15 **(2) Electrophoretic infiltration**

16  
17 **Vertical electrode:** Due to settling of the powder in the suspension, it was not possible to  
18  
19 achieve EPI successfully using vertical electrodes with powders coarser than 2.5  $\mu\text{m}$ ; the results  
20  
21 obtained using the finer powders for suspension B are shown in Table III and Fig. 7. Irrespective  
22  
23 of the particle sizes used, there was a clear trend as a function of the product of voltage and  
24  
25 time, Fig. 7, with increased deposition being achieved at higher voltages and longer times as  
26  
27 expected. However, for a given product of voltage  $\times$  time the 0.6  $\mu\text{m}$  particles resulted in greater  
28  
29 powder deposition than the 2.5  $\mu\text{m}$  particles (provided all layers within the tow were  
30  
31 impregnated), which in turn led to greater porosity reduction, Table III. In addition, the powder  
32  
33 deposition rate decreased as processing time increased, compare for example, E/5/25-100/30  
34  
35 and E/5/25-100/60 in Table III. This is also not surprising since the deposition rate is affected by  
36  
37 the particle concentration in the suspension. This will decrease as deposition progresses,  
38  
39 especially when the initial solids loading is low and the suspension is not stirred. Although the  
40  
41 effect of stirring was briefly investigated, it was found that the gain in mass was reduced  
42  
43 indicating that the movement of particles in the electric field was perturbed.  
44  
45  
46  
47  
48

49 SEM examination revealed that both sizes of powder deposited on the front surface of each  
50  
51 fabric layer forming a continuous film covering the exposed surface, with very little SiC powder  
52  
53 penetration within the fiber tows, Fig. 8a and 8b. As expected, the 0.6  $\mu\text{m}$  particles penetrated a  
54  
55 little further than the 2.5  $\mu\text{m}$  particles, however higher voltages resulted in less penetration.  
56  
57 Although this is perhaps counter-intuitive, higher voltages will have resulted in the particles  
58  
59  
60

1  
2  
3  
4  
5  
6 accumulating on the fabric surface more rapidly, consequently blocking the paths into the  
7 intratow porosity. Nevertheless, the powders were deposited with a high density in the intertow  
8 porosity, Fig. 8c, leaving relatively few unimpregnated regions after stacking the fabric layers to  
9 form the preforms, Fig. 8a. Despite this, the impregnated preforms were very weak and suffered  
10 delamination very easily, preventing gas permeabilities being measured.  
11  
12  
13  
14  
15  
16  
17

18 DEXA characterisation showed that the powder tended to form a 'crown' pattern around the  
19 centre, leaving the centre less impregnated than the periphery, Fig. 6b (the lack of deposition  
20 around the circumference arises from the presence of the polypropylene mask used to keep the  
21 fabric layer attached to the electrode). It is believed that this was caused by the lack of stirring  
22 during deposition resulting in sedimentation and hence preferential deposition at the bottom of  
23 each fabric layer attached to the electrode. Once randomly stacked up together, the 'crown'  
24 pattern was formed.  
25  
26  
27  
28  
29  
30  
31  
32  
33  
34

35 **Rotating electrode:** Since stirring the slurry reduced mass deposition by disturbing the motion  
36 of the particles within the suspension, a rotating electrode approach was investigated to improve  
37 the uniformity of the powder distribution across the fabric area. Whilst very little variation in the  
38 mass of powder deposited was observed in the range 0 to 6 rpm, a rotation of 3 rpm was found  
39 to be the optimum speed based on the uniformity of the powder deposition. This electrode  
40 proved to be more tolerant of stirring of the suspension and very low stirring speeds were found  
41 to benefit the uniformity of deposition on the fabric surface without significantly affecting the  
42 amount of powder deposited.  
43  
44  
45  
46  
47  
48  
49  
50  
51  
52

53 **Horizontal electrode:** The horizontal electrode arrangement enabled larger SiC particles to be  
54 deposited, indeed they benefited the process by adding a degree of gravitational settling and so,  
55 as expected, the masses deposited were slightly more than for the vertical electrode, Fig. 9.  
56  
57  
58  
59  
60

1  
2  
3  
4  
5  
6 They also resulted in less intratow penetration whilst continuing to achieve successful filling of  
7  
8 the intertow porosity. The most even distributions across the fabric surface were observed to  
9  
10 occur for deposition times of less than 90 s.  
11

12  
13  
14 When the horizontal electrode was used without the application of an electric field, i.e. pure  
15  
16 gravitational settling (GS), the mass of powder deposited was approximately halved but the  
17  
18 distribution of powder across the fabric surface was slightly more even and the intertow  
19  
20 macrovoids were efficiently filled, irrespective of the slurry used. This is presumably because the  
21  
22 slower deposition rate yielded a more uniform build up of powder.  
23  
24  
25

26  
27 Throughout the work using EPI, the ethanol-based slurry B took less time to dry, but resulted in  
28  
29 a greater degree of cracking and delamination of the preforms than the aqueous-based slurry C,  
30  
31 presumably because of the faster rate of solvent movement.  
32  
33

### 34 35 36 **(3) Combined processes**

37  
38 Table IV summarises the results obtained when powder was deposited on the fabric layers from  
39  
40 slurry C by EPI, using the horizontal electrode arrangement and 50 V for 60 s, and then the  
41  
42 resulting preforms were consolidated by VB. Very uniform powder deposition across the fabric  
43  
44 layers was observed, Fig. 6c, with the intertow porosity densely filled but almost no penetration  
45  
46 of the particles into the intratow porosity when the 6.7 and 10  $\mu\text{m}$  SiC particle sizes were used,  
47  
48 Fig. 10. The major advantage observed for this technique was the ability to produce relatively  
49  
50 strong and well compacted preforms from the VB stage of the process, with high densities as a  
51  
52 result of the EPI process, but without the SiC particles filling the intratow voids when the coarser  
53  
54 SiC particles were used. Despite the higher densities, the gas permeabilities were a factor of 3 –  
55  
56 6 higher than for the VB route on its own supporting the view that the intratow gas channels, so  
57  
58 important for CVI, had not become blocked.  
59  
60

1  
2  
3  
4  
5  
6  
7  
8  
9  
10  
11  
12  
13  
14  
15  
16  
17  
18  
19  
20  
21  
22  
23  
24  
25  
26  
27  
28  
29  
30  
31  
32  
33  
34  
35  
36  
37  
38  
39  
40  
41  
42  
43  
44  
45  
46  
47  
48  
49  
50  
51  
52  
53  
54  
55  
56  
57  
58  
59  
60

Table IV also shows the results obtained when gravitational settling of the SiC particles was used to coat the fabric layers using the horizontal electrode but without any electric field and then the preforms were consolidated using the VB process. Once again, the powder distribution across the preform diameter was uniform, the intertow porosity was densely filled and the intratow porosity remained largely empty. Although the gas permeability was similar for the combined EPI/VB process for the aqueous slurry C, when the ethanol-based slurry B was used the value was approximately doubled to almost that of the unimpregnated preforms.

#### IV Conclusions

Both the VB and EPI processes led to the impregnation of SiC fabric preforms with SiC powders, although the distribution of the powder was significantly different in the two cases, affecting both the strength and gas permeability of the final preforms. With the VB process, the SiC powder was forced into the intratow porosity and only filled the intertow porosity if the solids content of the suspension was sufficiently high; the opposite of what was required. In addition, the process relied on the manual brushing of the suspension onto the fabric disks; a process that led to a degree of variability despite attempts to control it. Much more uniform, controllable and reproducible deposition was achieved with the EPI process, with the intertow porosity being filled particularly densely but relatively little penetration of the particles into the intratow porosity, particularly when larger SiC particles were used. To avoid non-uniform distribution of the particles across the SiC fabric layers, a horizontal electrode arrangement was developed. This actually yielded slightly superior preforms when the electric field was turned off and gravity alone used to achieve deposition, although the time required obviously increased.

The main problem with the EPI process was that the resulting preforms were particularly weak and delaminated easily during handling. In contrast, the VB-formed preforms were relatively

1  
2  
3  
4  
5  
6 strong. The combination of EPI using a horizontal electrode, with or without the electric field  
7  
8 switched on, followed by VB yielded strong preforms with a high degree of powder loading but  
9  
10 which also retained a high level of gas permeability, a major requirement for the subsequent CVI  
11  
12 stage.  
13

### 14 15 16 **Acknowledgements**

17  
18 The authors would like to acknowledge funding by QinetiQ Ltd (formerly the Defence Evaluation  
19  
20 Research Agency (DERA) of the UK.  
21  
22  
23  
24  
25  
26  
27  
28  
29  
30  
31  
32  
33  
34  
35  
36  
37  
38  
39  
40  
41  
42  
43  
44  
45  
46  
47  
48  
49  
50  
51  
52  
53  
54  
55  
56  
57  
58  
59  
60

## References

1. T. M. Besmann, B. W. Sheldon, R. A. Lowden and D. P. Stinton, "Vapor-phase fabrication and properties of continuous-filament ceramic composites", *Science* **253** 1104-1109 (1991).
2. R. Naslain, "Design, preparation and properties of non-oxide CMCs for application in engines and nuclear reactors: an overview", *Comp. Sci. and Techn.* **64** 155-170 (2004).
3. D. Brewer, "HSR/EPM combustor materials development program", *Mater. Sci. Eng.* **A261** 284-291 (1999).
4. K. J. Probst., T. M. Besmann., D. P. Stinton, R. A. Lowden, T. J. Anderson and T.L. Starr, "Recent advances in forced-flow, thermal-gradient CVI for refractory composites", *Surfaces and Coatings Techn.* **120-121** 250-258 (1999).
5. B.W.Sheldon, "The control of gas phase kinetics to maximize densification during chemical vapour infiltration", *J. Mater. Res.* **5** [11] 2729-2736 (1990).
6. S. Bertrand., J. F. Lavaud, R. El Hadi, G. Vignoles and R. Pailler, "The thermal gradient-pulse flow CVI process: a new chemical vapour infiltration technique for the densification of fibre preforms", *J. Eur. Ceram. Soc.* **18** 857-870 (1998).
7. J.H. Kinney, T.M. Breunig, T.L. Starr, D. Haupt, M.C. Nichols, S.R. Stock, M.D. Butts and R.A. Saroyan, "X-ray tomographic study of chemical vapour infiltration processing of ceramic composites", *Science* **260** 789-791 (1993).
8. J.Y. Ofori and S.V. Sotirchos, "Dynamic convection-driven thermal gradient chemical vapour infiltration", *J. Mater. Res.* **11** [10] 2541-2555 (1996).
9. D. J. Skamser, J. J. Thomas, H.M. Jennings and D.L. Johnson, "Microwave heating of a changing material", *Ceram. Trans.* **59** 289-298 (1995).
10. A. Ortona, A. Donato, G. Filacchioni, U. De Angelis, A. La Barbera, C. A. Nannetti, B. Riccardi and J. Yeatman, "SiC-SiC<sub>f</sub> CMC manufacturing by hybrid CVI-PIP techniques:

- process optimisation”, *Fusion Eng. and Design* **51-52** 159-163 (2000).
11. D. Jaglin, J. Binner, B. Vaidyanathan, C. Prentice, R.A. Shatwell and D.G. Grant, “Microwave heated chemical vapour infiltration: Densification mechanism of SiC<sub>f</sub>/SiC Composites”, *J. Am. Ceram. Soc.* **89** [9] 2710-2717 (2006).
  12. R.J. Shinavski and R.J. Diefendorf, “CVI processing of thin C/HfB<sub>2</sub> composites”, *Ceram. Eng. Sci. Proc.* **14** [9/10] 824-831 (1993).
  13. M. Jones and T.L. Starr, “Enhancements to the Georgia Tech. chemical vapour infiltration process model for ceramic matrix composites”, *Ceram. Eng. Sci. Proc.* **16** [5] 829-836 (1995).
  14. W.J. Lackey, S. Vaidyaraman, G.B. Freeman and P.K. Agrawal, “Technique for monitoring densification during chemical vapour infiltration”, *J. Am. Ceram. Soc.* **78** [4] 1131-1133 (1995).
  15. T. Yano, K. Budiyo, K. Yoshida and T. Iseki, “Fabrication of silicon carbide fiber-reinforced silicon carbide composite by hot-pressing”, *Fusion Eng. and Design* **41** 157-163 (1998).
  16. A. Sayano, C. Sutoh, S. Suyama, Y. Itoh and S. Nakagawa, “Development of a reaction-sintered silicon carbide matrix composite”, *J. Nucl. Mater.* **271-272** 467-471 (1999).
  17. J. J. Brennan, “Interfacial characterization of a slurry-cast melt-infiltrated SiC/SiC ceramic-matrix composite”, *Acta Mater.* **48** 4619-4628 (2000).
  18. D. Brewer, “HSR/EPM combustor materials development program”, *Mater. Sci. Eng.* **A261** 284291 (1999).
  19. H. O. Davies and D. R. Petrak, “Ceramic matrix composites using polymer pyrolysis and liquid densification processing”, *J. Nucl. Mater.* **219** 26-30 (1995).

- 1  
2  
3  
4  
5  
6 20. J. Gotoh, K. Tsugeki, A. Sakai and H. Nakayama, "Fabrication and mechanical properties of  
7 ceramic matrix composites by polymer impregnation and pyrolysis method", *Proc. 4<sup>th</sup> Japan*  
8 *Int. SAMPE Symp.* pp. 240-245 (1995).  
9  
10  
11  
12  
13 21. M.F. Gonon and S. Hampshire, "Comparison of two processes for manufacturing ceramic  
14 matrix composites from organometallic precursors", *J. Eur. Ceram. Soc.* **19** 285-291 (1999).  
15  
16  
17 22. Y-W. Kim, J-S. Song, S-W. Park and J-G. Lee, "Nicalon-fibre-reinforced silicon-carbide  
18 composites via polymer solution infiltration and chemical vapour infiltration", *J. Mater. Sci.*  
19 **28** 3866-3868, (1993.)  
20  
21  
22  
23 23. S. Casadio, A. Donato, C.A. Nannetti, A. Ortona and M. Rescio, "Liquid infiltration and  
24 pyrolysis of SiC matrix composite materials", *Ceram. Trans.* **58** 193-198 (1995).  
25  
26  
27  
28 24. S. M. Dong, Y. Katoh, A. Kohyama, S. T. Schwab and L. L. Snead, "Microstructural  
29 evolution and mechanical performances of SiC/SiC composites by polymer  
30 impregnation/microwave pyrolysis (PIMP) process", *Ceram. Int.* **28** 899-905 (2002).  
31  
32  
33  
34 25. G. Ziegler, I. Ritcher and D. Suttor, "Fiber-reinforced composites with polymer-derived  
35 matrix: processing matrix formation and properties", *Composites: Part A* **30** 411-417 (1999).  
36  
37  
38  
39 26. G.R. Sherwin, "Non-autoclave processing of advanced composite repairs", *Int. J. of*  
40 *Adhesion & Adhesives* **19** 155-159 (1999).  
41  
42  
43  
44 27. G. Sala, "Advances in elastomeric tooling technology", *Materials & Design* **17** [1] 33-42  
45 (1996).  
46  
47  
48  
49 28. M.Z. Berbon, D.R. Dietrich, D.B. Marshall and D.P.H. Hasselman, "Transverse thermal  
50 conductivity of thin C/SiC composites fabricated by slurry infiltration and pyrolysis", *J. Am.*  
51 *Ceram. Soc.* **84** [10] 2229-2234 (2001).  
52  
53  
54  
55 29. A. Timms, W. Westby, C. Prentice, D. Jaglin, R. A. Shatwell and J. G. Binner, "Reducing  
56 chemical vapour infiltration time for ceramic matrix composites", *J. Microsc.*, **201-202** 316-  
57  
58  
59  
60



- 1  
2  
3  
4  
5  
6 323 (2001).  
7  
8  
9 30. P. Sarkar, S. Datta and P.S. Nicholson, "Functionally graded ceramic/ceramic and  
10 metal/ceramic composites by electrophoretic deposition", *Composites Part B* **28B** 49-56  
11 (1997).  
12  
13  
14  
15 31. S.N. Heavens, "Electrophoretic deposition as a processing route for ceramics", *Advanced*  
16 *Ceramic Processing & Technology Vol. 1*, pp. 255-283, Ed. J.G.P. Binner, Noyes  
17 Publications (1990).  
18  
19  
20  
21  
22 32. A.R. Boccaccini, I. MacLaren and M.H. Lewis, "Electrophoretic deposition infiltration of 2-D  
23 woven SiC fibre mats with mixed sols of mullite composition", *J. Eur. Ceram. Soc.* **17** 1545-  
24 1550 (1997).  
25  
26  
27  
28  
29 33. A. Borner and R. Herbig, "ESA measurement for electrophoretic deposition of ceramic  
30 materials", *Colloids and Surfaces A: Physicochemical and Engineering Aspects* **159** 439-  
31 447 (1999).  
32  
33  
34  
35  
36 34. H.H. Streckert and J.D. Katz, "Microwave densification of electrophoretically infiltrated  
37 silicon carbide composite", *J. Mater. Sci.* **32** 6429-6433 (1997).  
38  
39  
40  
41 35. S. Kooner, J.J. Campaniello S., Pickering and E. Bullock, "Fiber reinforced ceramic matrix  
42 composite fabrication by electrophoretic infiltration", *Ceram. Trans.* **58** 155-160 (1995).  
43  
44  
45 36. D. Jaglin, J. Binner, C. Prentice, R. Shatwell, L. Timms and W. Westby, "SiC<sub>f</sub>/SiC fabrication  
46 via vacuum bagging, electrophoretic infiltration and microwave enhanced CVI", 9<sup>th</sup> Eur.  
47 Conf. on Composite Materials (ECCM 9) proceedings CD, Institute of Materials, Minerals and  
48 Mining, UK (2000).  
49  
50  
51  
52  
53 37. A. P. Philipse, "Non-darcian airflow through ceramic foams", *J. Am. Ceram. Soc.*, **74** [4] 728-  
54 732 (1991).  
55  
56  
57  
58  
59  
60

- 1  
2  
3  
4  
5  
6  
7  
8  
9  
10  
11  
12  
13  
14  
15  
16  
17  
18  
19  
20  
21  
22  
23  
24  
25  
26  
27  
28  
29  
30  
31  
32  
33  
34  
35  
36  
37  
38  
39  
40  
41  
42  
43  
44  
45  
46  
47  
48  
49  
50  
51  
52  
53  
54  
55  
56  
57  
58  
59  
60
38. T. L. Starr and N. Hablutzel, "Measurement of gas transport through fiber preforms and densified composites for chemical vapour infiltration," *J. Am. Ceram. Soc.* **81** [5] 1298–304 (1998).
39. J. Binner, B. Vaidhyanathan and D. Jaglin, "Microwave heated chemical vapour infiltration of SiC powder impregnated SiC fibre preforms", *Advances in Applied Ceramics: Structural, Functional and Bioceramics, In Press.*

For Peer Review

## Captions

Fig. 1: SEM images of SiC<sub>r</sub>/SiC composites processed by CVI (a) low magnification showing large intertow voids and (b) high magnification showing fine intratow porosity. 72 x 72 dpi

Fig. 2: Schematic diagrams showing (a) the vacuum bagging equipment and (b) the electrophoretic impregnation system. 72 x 72 dpi

Fig. 3: Design variations for the anode used for EPI of SiC powder from suspension onto SiC fabric layers. 72 x 72 dpi

Fig. 4a: Reduction in porosity observed in the VB preforms as a function of the solids loading in the SiC slurries. 72 x 72 dpi

Fig. 4b: Reduction in porosity observed in the VB preforms as a function of the particle size in the SiC slurries. 72 x 72 dpi

Fig. 5: SEM cross sectional micrographs of preforms prepared by VB at two different magnifications (a) and (c) V/30/6, (b) and (d) V/20/6. 72 x 72 dpi

Fig. 6: Colour enhanced DEXA scans for samples prepared by a) VB, b) EPI using the vertical electrode and c) combined VB and EPI using the horizontal electrode. 72 x 72 dpi

Fig. 7: Reduction in porosity versus (voltage x time) applied during the EPI process using the vertical electrode. 72 x 72 dpi

1  
2  
3  
4  
5  
6 Fig. 8: Low and high magnification SEM images of cross sections of preforms formed by EPI (a)  
7  
8 and (b) E/5/6-50/90† and (c) E/5/6-100/45. 72 x 72 dpi  
9

10  
11  
12 Fig. 9: Reduction in porosity versus deposition time for EPI using the vertical (V) and horizontal  
13  
14 (H) electrodes and different SiC particle sizes. 72 x 72 dpi  
15  
16

17  
18 Fig. 10: Low and high magnification SEM images of cross sections of preforms formed by  
19  
20 combined VB and EPI (a) and (b) EV/5/25-50/60; (c) and (d) EV/5/67-50/60 and (e) and (f)  
21  
22 EV/5/100-50/60. 72 x 72 dpi  
23  
24  
25  
26  
27  
28  
29  
30

31 Table I: Mean particle size and source of SiC particles used.  
32  
33

34  
35 Table II: Impregnation results achieved by the VB process.  
36  
37  
38

39  
40 Table III: Impregnation results achieved by the EPI process.  
41  
42  
43

44 Table IV: Impregnation results achieved by the combined horizontal EPI and VB processes and  
45  
46 the combined horizontal GS and VB processes.  
47  
48  
49  
50  
51  
52  
53  
54  
55  
56  
57  
58  
59  
60

Table I: Mean particle size and source of SiC particles used.

| Mean particle size / $\mu\text{m}$ | Source  |
|------------------------------------|---|
| 0.6                                | UF15, HC Starck, Goslar, Germany  |
| 2.5                                | ESK1500F, ESK, Kempten, Germany   |
| 6.7                                | Reliable Techniques, Newcastle-under-Lyme, UK                                 |
| 10.0                               | Carborex BW Micro F 600 PV, Washington Mills Electro Minerals, Manchester, UK |
| 12.8                               | Silkaride CS F1200, Washington Mills Electro Minerals, Manchester, UK         |

Table II: Impregnation results achieved by the VB process.

| Sample   | Slurry type | Solid loading / % | Particle size / $\mu\text{m}$ | $V_f$ / % | $V_p$ / % | V.R. / % | Relative density / % | Gas permeability <sup>#</sup> / $10^{-12} \text{ m}^2$ |
|----------|-------------|-------------------|-------------------------------|-----------|-----------|----------|----------------------|--|
| V/20/6   | A           | 20                | 0.6                           | 25        | 9         | 12       | 34                   | *  |
| V/20/25  | A           | 20                | 2.5                           | 23        | 6         | 10       | 29                   | *  |
| V/20/128 | A           | 20                | 12.8                          | 21        | 8         | 11       | 29                   | *  |
| V/30/6   | A           | 30                | 0.6                           | 35        | 15        | 23       | 50                   | *  |
| V/30/100 | A           | 30                | 10.0                          | 14        | 15        | 17       | 29                   | 1.3  |
| V/35/6   | A           | 35                | 0.6                           | 21        | 18        | 23       | 39                   | 2.0  |
| V/35/25  | A           | 35                | 2.5                           | 19        | 16        | 28       | 35                   | 1.9  |
| V/35/67  | A           | 35                | 6.7                           | 16        | 19        | 23       | 35                   | 1.8  |
| V/35/100 | A           | 35                | 10.0                          | 18        | 21        | 26       | 39                   | 1.1  |
| V/40/100 | A           | 40                | 10.0                          | 16        | 21        | 25       | 37                   | 1.0  |

<sup>#</sup> $16 \times 10^{-12} \text{ m}^2$  for a powderless preform

\*Technique not available at the time

Table III: Impregnation results achieved by the EPI process.

| Sample                   | Slurry type | Solid loading / % | Particle size / $\mu\text{m}$ | Electrode type | Voltage / V | Time / s | $V_f$ / % | $V_p$ / % | V.R. / % | Relative density / % |
|--------------------------|-------------|-------------------|-------------------------------|----------------|-------------|----------|-----------|-----------|----------|----------------------|
| E/5/6-50/45 <sup>†</sup> | B           | 5                 | 0.6                           | Vertical       | 50          | 45       | 21        | 7         | 9        | 28                   |
| E/5/6-50/60              | B           | 5                 | 0.6                           | Vertical       | 50          | 60       | 17        | 15        | 18       | 32                   |
| E/5/6-50/90              | B           | 5                 | 0.6                           | Vertical       | 50          | 90       | 16        | 18        | 21       | 34                   |
| E/5/6-50/90 <sup>†</sup> | B           | 5                 | 0.6                           | Vertical       | 50          | 90       | 22        | 12        | 15       | 34                   |
| E/5/6-100/45             | B           | 5                 | 0.6                           | Vertical       | 100         | 45       | 20        | 19        | 24       | 39                   |
| E/5/25-50/60             | B           | 5                 | 2.5                           | Vertical       | 50          | 60       | 20        | 11        | 14       | 31                   |
| E/5/25-100/30            | B           | 5                 | 2.5                           | Vertical       | 100         | 30       | 22        | 13        | 17       | 35                   |
| E/5/25-100/60            | B           | 5                 | 2.5                           | Vertical       | 100         | 60       | 19        | 21        | 26       | 40                   |
| E/10/25-50/60            | B           | 10                | 2.5                           | Vertical       | 50          | 60       | 18        | 26        | 32       | 44                   |
| E/5/25-50/60             | B           | 5                 | 2.5                           | Horizontal     | 50          | 60       | 18        | 12        | 15       | 30                   |

<sup>†</sup> Alternate layers impregnated

Table IV: Impregnation results achieved by the combined horizontal EPI and VB processes and the combined horizontal GS and VB processes.

| Sample         | Slurry type | Solid loading / % | Particle size / $\mu\text{m}$ | $V_f$ / % | $V_p$ / % | V.R. / % | Relative density / % | Gas permeability / $10^{-12} \text{ m}^2$ |
|----------------|-------------|-------------------|-------------------------------|-----------|-----------|----------|----------------------|---|
| EV/5/25-50/60  | C           | 5                 | 2.5                           | 18        | 17        | 21       | 35                   | 6.9                                       |
| EV/5/67-50/60  | C           | 5                 | 6.7                           | 21        | 18        | 23       | 39                   | 6.8                                       |
| EV/5/100-50/60 | C           | 5                 | 10                            | 21        | 19        | 24       | 40                   | 6.3                                       |
| GV/5/67-B      | B           | 5                 | 6.7                           | 17        | 19        | 23       | 36                   | 12.8                                      |
| GV/5/67-C      | C           | 5                 | 6.7                           | 19        | 22        | 27       | 41                   | 6.8                                       |
| GV/5/100-B     | B           | 5                 | 10                            | 21        | 20        | 25       | 41                   | 10.6                                      |
| GV/5/100-C     | C           | 5                 | 10                            | 20        | 20        | 25       | 40                   | 6.0                                       |

1  
2  
3  
4  
5  
6  
7  
8  
9  
10  
11  
12  
13  
14  
15  
16  
17  
18  
19  
20  
21  
22  
23  
24  
25  
26  
27  
28  
29  
30  
31  
32  
33  
34  
35  
36  
37  
38  
39  
40  
41  
42  
43  
44  
45  
46  
47  
48  
49  
50  
51  
52  
53  
54  
55  
56  
57  
58  
59  
60

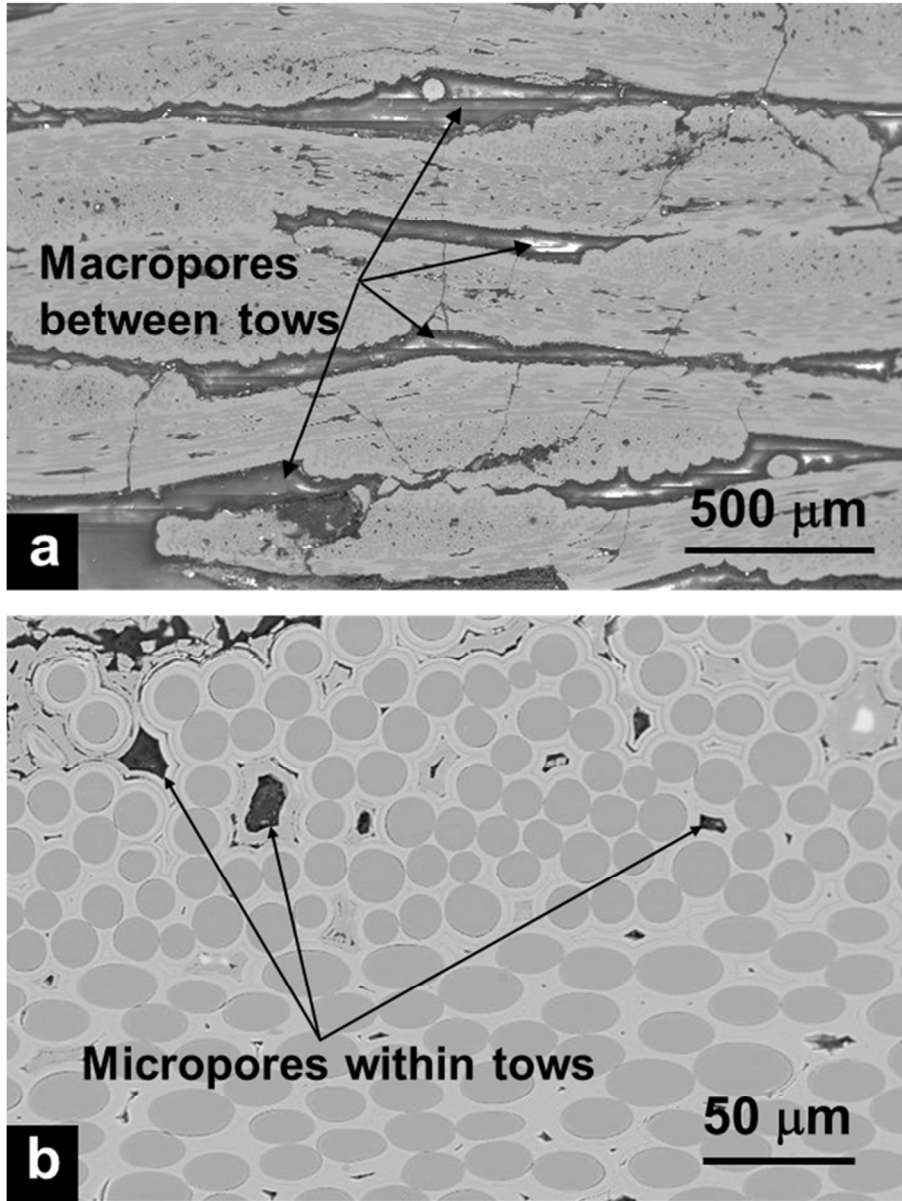


Fig 1. SEM images of SiCf/SiC composites processed by CVI (a) low magnification showing large intertow voids and (b) high magnification showing fine intratow porosity. 72 x 72 dpi

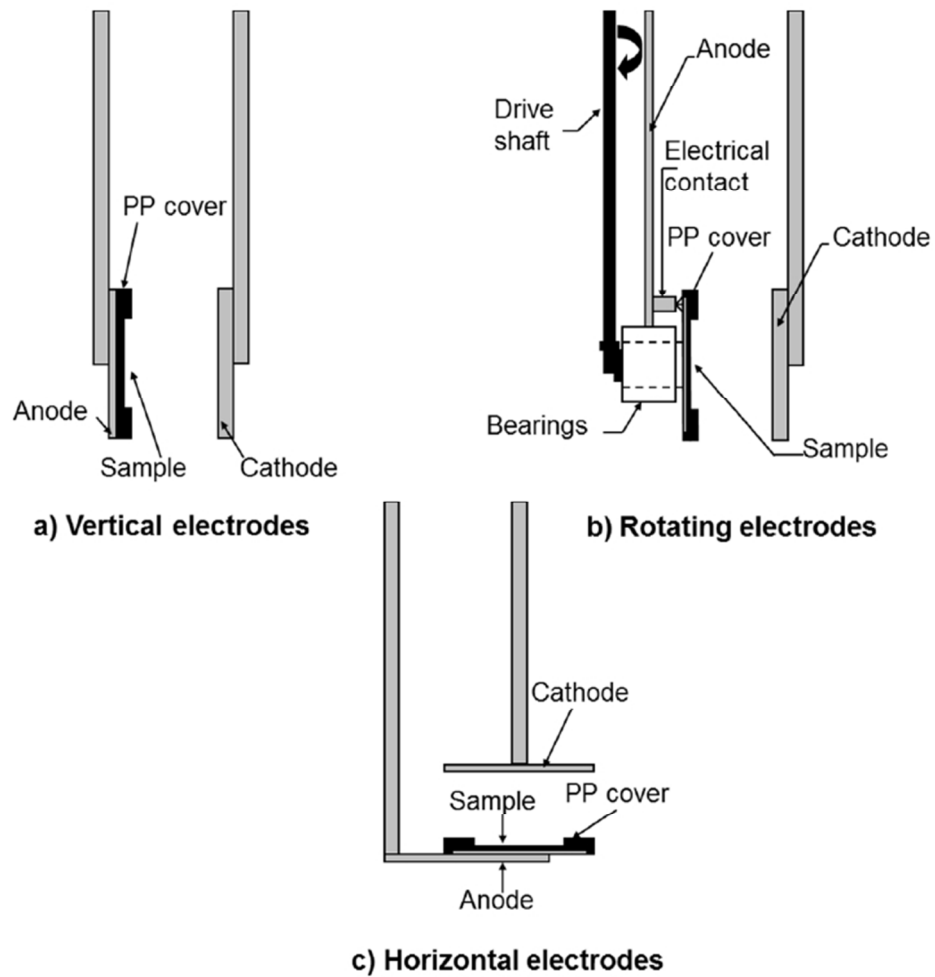
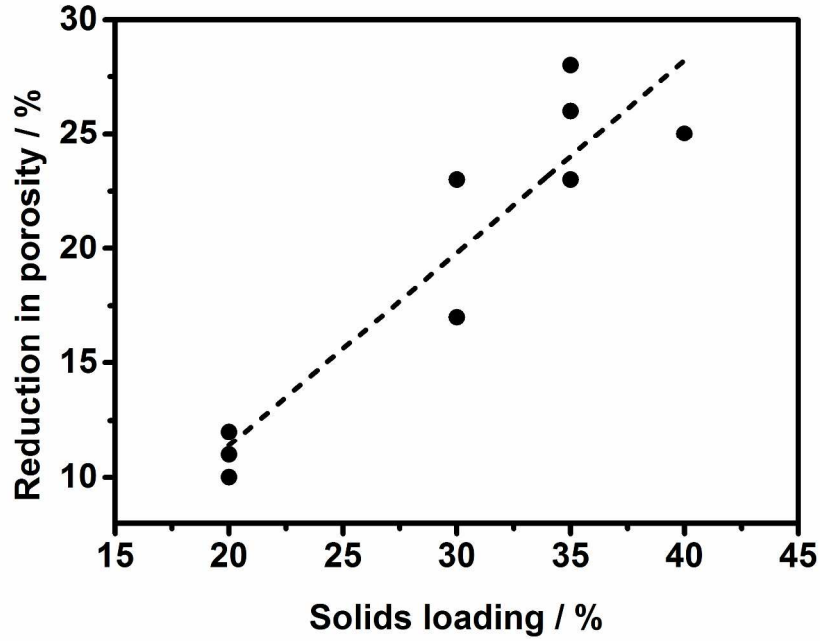


Fig 3. Design variations for the anode used for EPI of SiC powder from suspension onto SiC fabric layers. 72 x 72 dpi

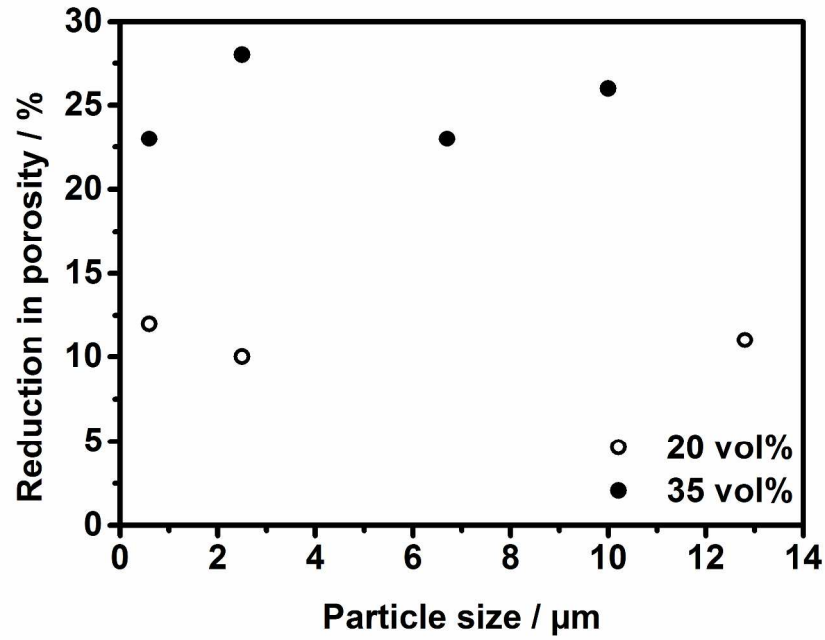


1  
2  
3  
4  
5  
6  
7  
8  
9  
10  
11  
12  
13  
14  
15  
16  
17  
18  
19  
20  
21  
22  
23  
24  
25  
26  
27  
28  
29  
30  
31  
32  
33  
34  
35  
36  
37  
38  
39  
40  
41  
42  
43  
44  
45  
46  
47  
48  
49  
50  
51  
52  
53  
54  
55  
56  
57  
58  
59  
60



Reduction in porosity observed in the VB preforms as a function of the solids loading in the SiC slurries. 72 x 287x201mm (300 x 300 DPI)

Review



Reduction in porosity observed in the VB preforms as a function of the particle size in the SiC slurries. 72 x 287x201mm (300 x 300 DPI)

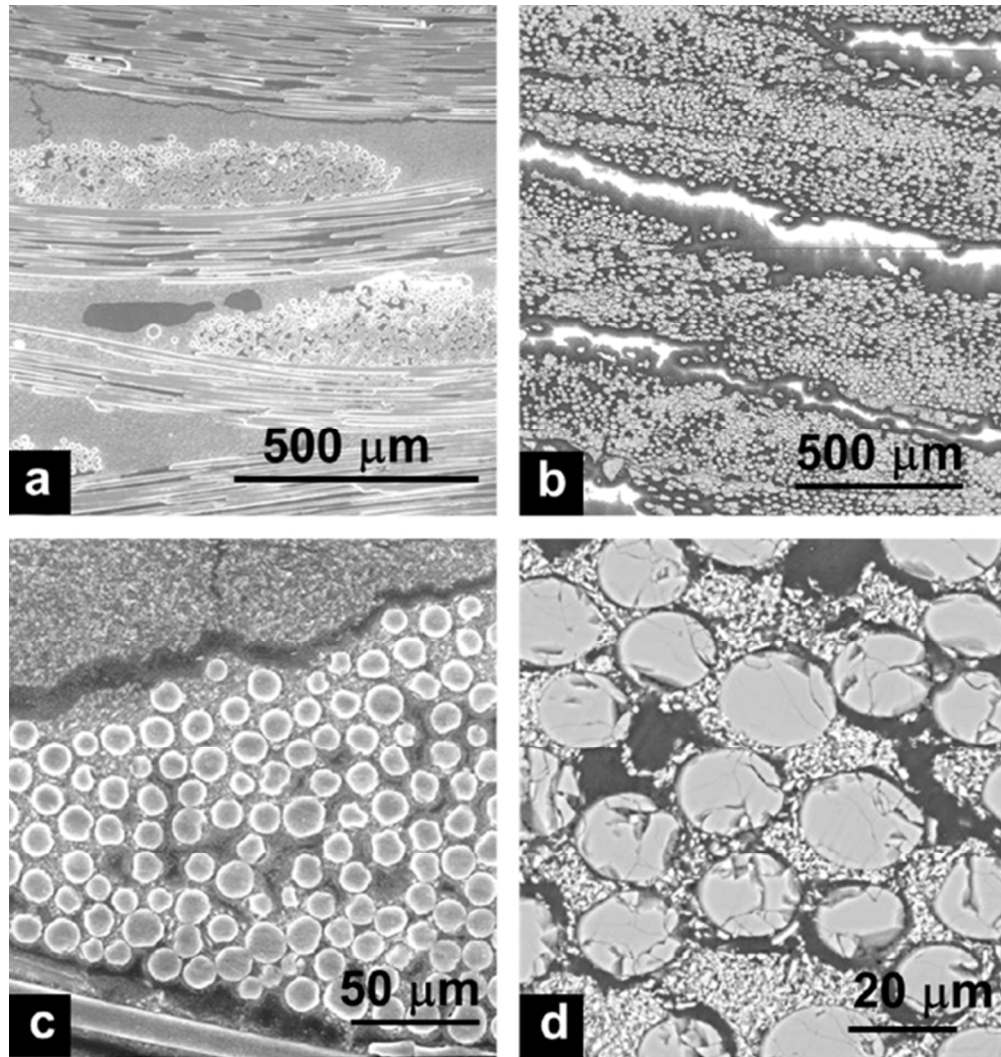


Fig 5. SEM cross sectional micrographs of preforms prepared by VB at two different magnifications (a) and (c) V/30/6, (b) and (d) V/20/6. 72 x 72 dpi

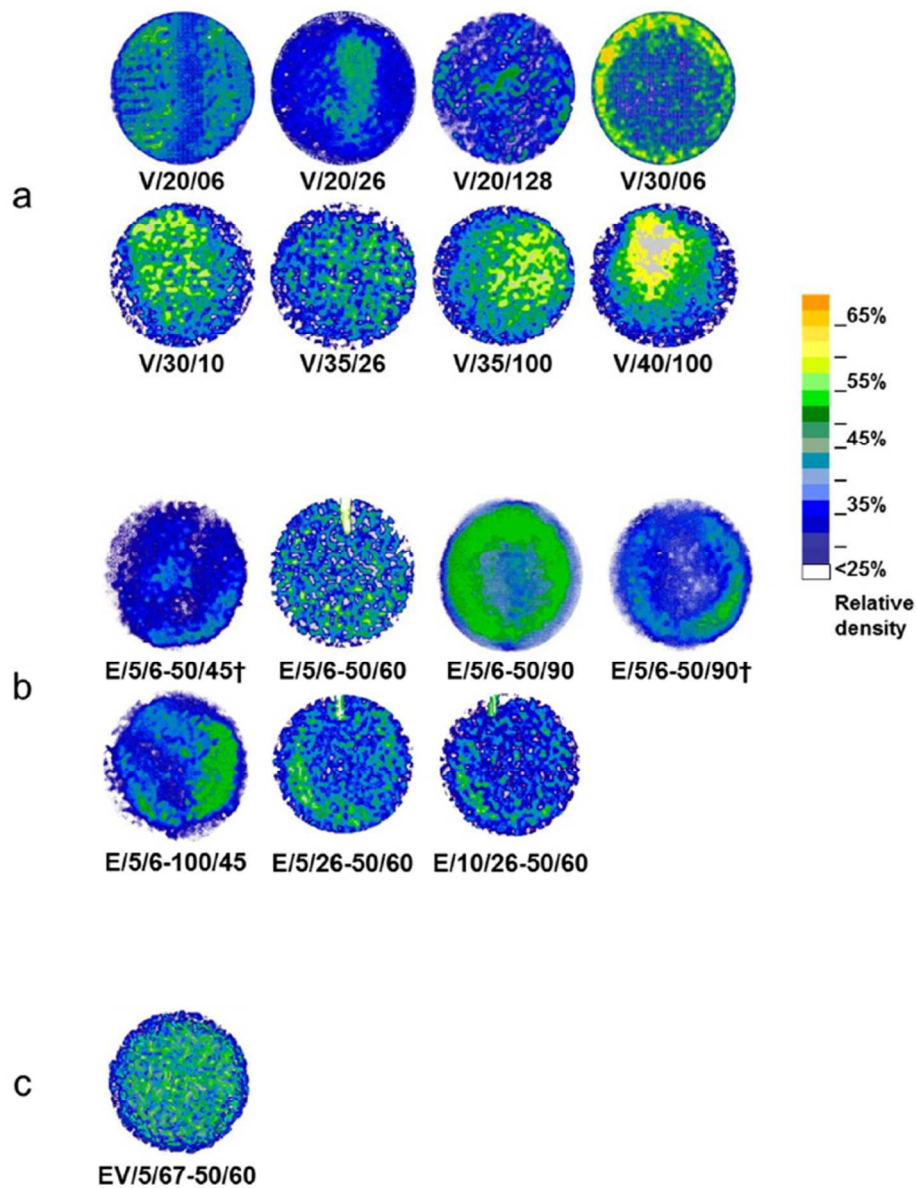
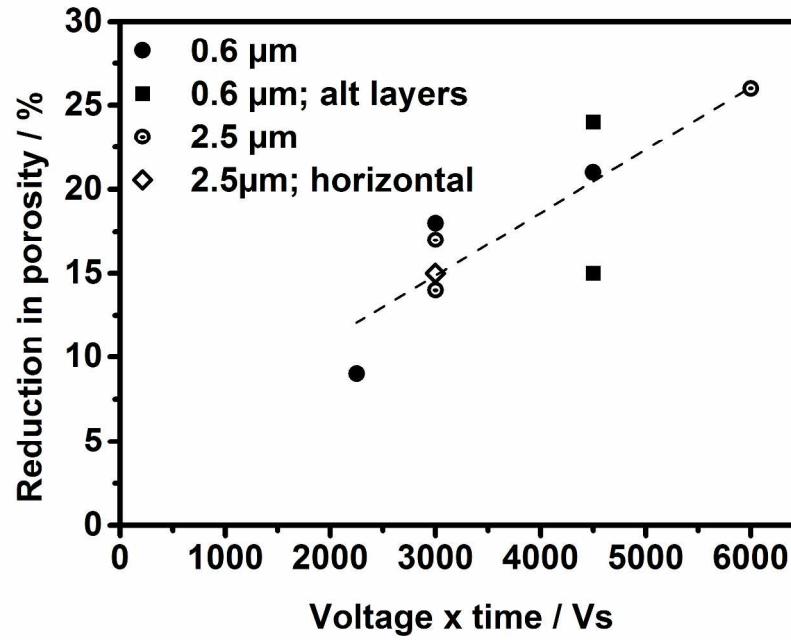


Fig 6. Colour enhanced XRA scans for samples prepared by a) VB, b) EPI using the vertical electrode and c) combined VB and EPI using the horizontal electrode. 72 x 72 dpi



Reduction in porosity versus (voltage×time) applied during the EPI process using the vertical electrode. 72 x  
72 dpi  
287x201mm (300 x 300 DPI)

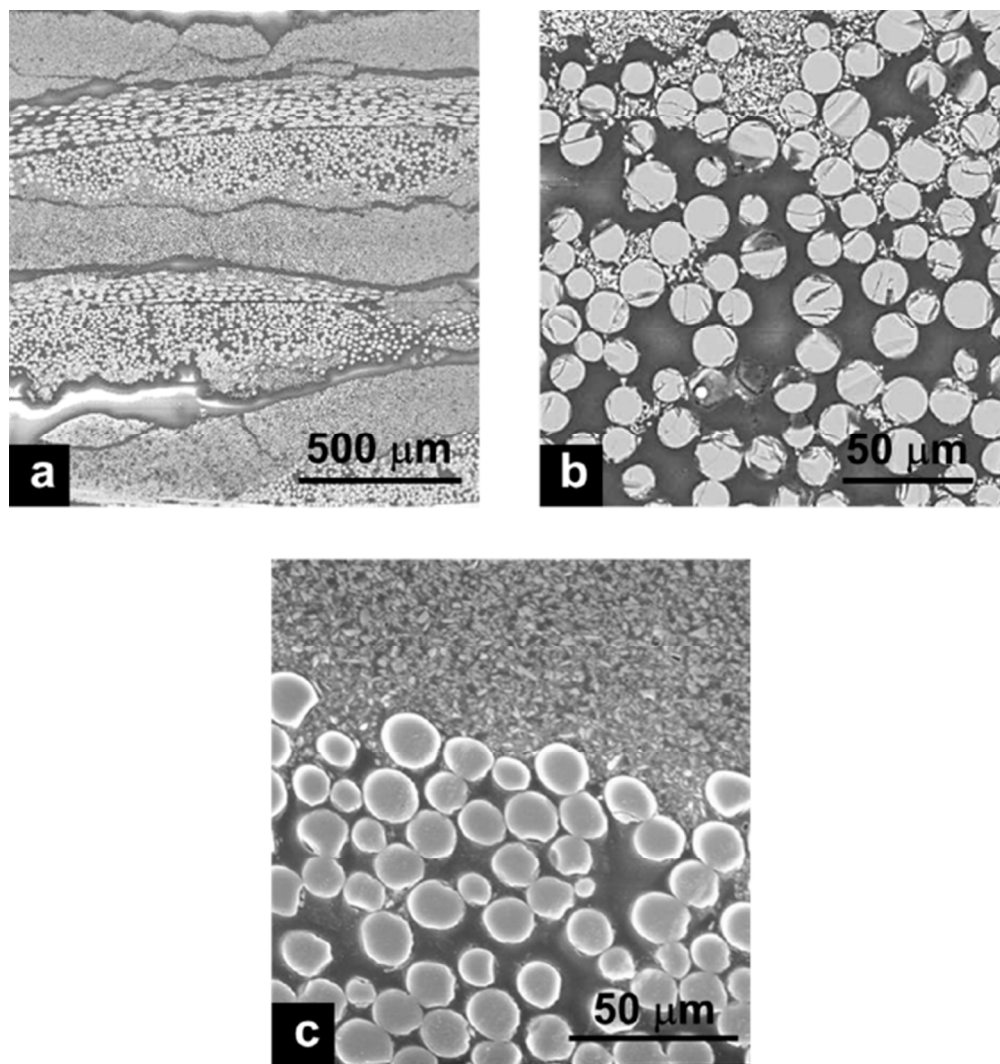
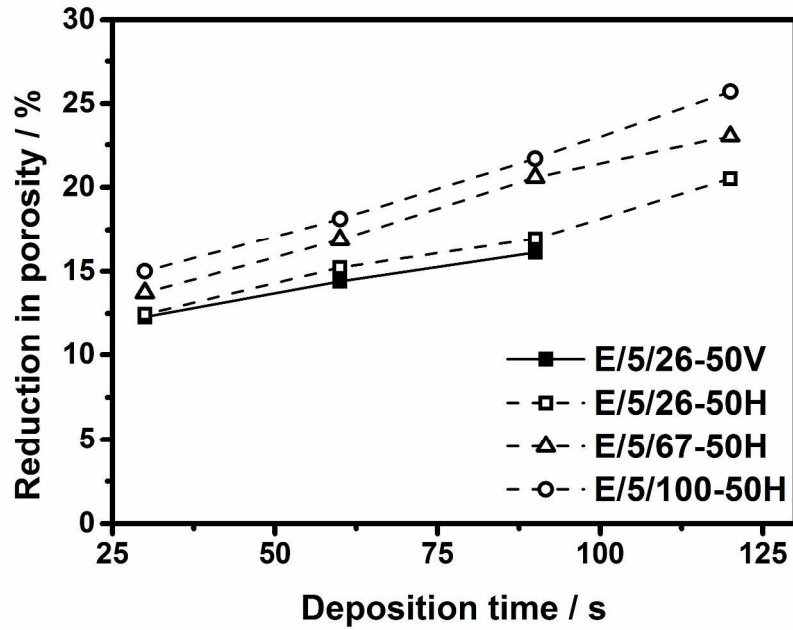


Fig 8. Low and high magnification SEM images of cross sections of preforms formed by EPI (a) and (b) E/5/6-50/90<sup>+</sup> and (c) E/5/6-100/45. 72 x 72 dpi



Reduction in porosity versus deposition time for EPI using the vertical (V) and horizontal (H) electrodes and different SiC particle sizes. 72 x 72 dpi  
287x201mm (300 x 300 DPI)



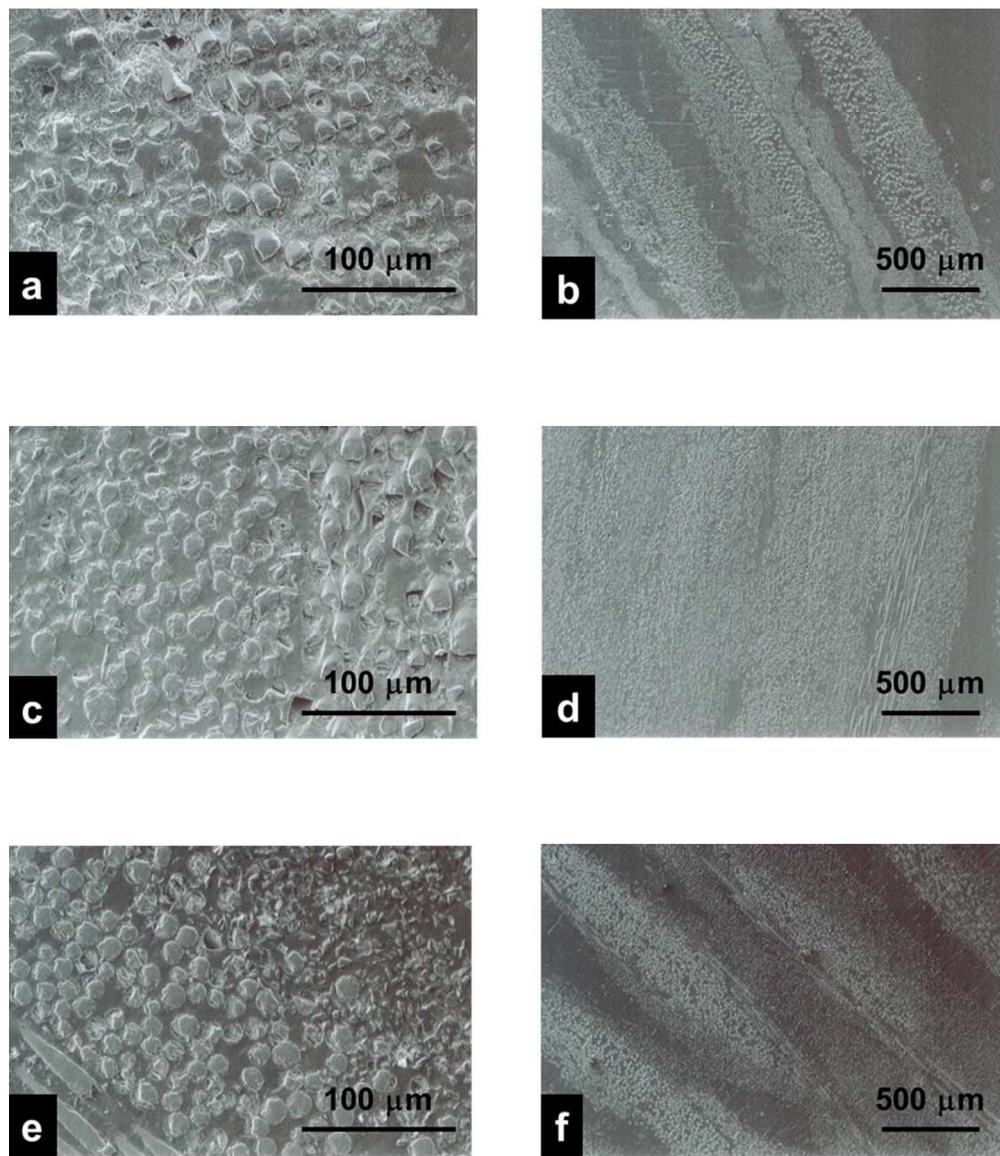


Fig 10. Low and high magnification SEM images of cross sections of preforms formed by combined VB and EPI (a) and (b) EV/5/25-50/60; (c) and (d) EV/5/67-50/60 and (e) and (f) EV/5/100-50/60. 72 x 72 dpi